Chapter 9

LONGITUDINAL COUPLED-BUNCH INSTABILITIES

When the wake does not decay within the bunch spacing, bunches talk to each other. Assuming M bunches of equal intensity equally spaced in the accelerator ring, there are $\mu = 0,\ 1,\ \cdots,\ M-1$ modes of oscillations in which the center-of-mass of a bunch *leads** its predecessor by the phase $2\pi\mu/M$. In addition, an individual bunch in the μth coupled-bunch mode can oscillate in the synchrotron phase space about its center-of-mass in the mth azimuthal mode with $2m = 2,\ 4,\ \cdots$ azimuthal nodes† in the perturbed longitudinal phase-space distribution. Of course, there will be in addition radial modes of oscillation in the perturbed distribution. The long-range wake can drive the coupled bunches to instability.

9.1 Sacherer's Integral Equation

Because the beam particles execute synchrotron oscillations, it is more convenient to use circular coordinates r, ϕ in the longitudinal phase space instead of the former time

*We can also formulate the problem by having the bunch *lag* its predecessor by the phase $2\pi\mu'/M$ in the μ'th coupling mode. Then mode μ' will be exactly the same as mode $M-\mu$ discussed in the text.

†For example, the dipole mode $m = 1$ can be written as $\sim \cos\phi$, which has two nodes $\phi = \pm\pi/2$.

advance τ and energy offset ΔE. We define

$$\begin{cases} x &= r\cos\phi = \tau \ , \\ p_x &= r\sin\phi = \dfrac{\eta}{\omega_s\beta^2}\dfrac{\Delta E}{E_0} \ , \end{cases} \tag{9.1}$$

so that the equations of motion

$$\begin{cases} \dfrac{dx}{ds} &= -\dfrac{\omega_s}{v}p_x \ , \\ \dfrac{dp_x}{ds} &= \dfrac{\omega_s}{v}x + \dfrac{\eta}{E_0\omega_s\beta^2}\langle F_0^{\parallel}(\tau;s)\rangle \ , \end{cases} \tag{9.2}$$

become more symmetric. In the absence of the wake force $\langle F_0^{\parallel}(\tau;s)\rangle$, the trajectory of a beam particle is just a circle in the longitudinal phase space. In above, ω_s is the angular small-amplitude synchrotron frequency, η the slip factor, and $v = \beta c$ is the velocity and E_0 the energy of the synchronous particle. The phase-space distribution ψ of a bunch can be separated into the unperturbed or stationary part ψ_0 and the perturbed part ψ_1:

$$\psi(\tau, \Delta E; s) = \psi_0(\tau, \Delta E) + \psi_1(\tau, \Delta E; s) \ . \tag{9.3}$$

The linearized Vlasov equation becomes

$$\frac{\partial\psi_1}{\partial s} - \frac{\omega_s}{v}p_x\frac{\partial\psi_1}{\partial x} + \frac{\omega_s}{v}x\frac{\partial\psi_1}{\partial p_x} + \frac{\partial\psi_0}{\partial p_x}\frac{\eta}{E_0\omega_s\beta^2}\langle F_0^{\parallel}(\tau;s)\rangle = 0 \ . \tag{9.4}$$

Changing to the circular coordinates, the equation simplifies to

$$\frac{\partial\psi_1}{\partial s} + \frac{\omega_s}{v}\frac{\partial\psi_1}{\partial\phi} + \frac{\eta}{E_0\omega_s\beta^2}\frac{d\psi_0}{dr}\sin\phi\langle F_0^{\parallel}(\tau;s)\rangle = 0 \ . \tag{9.5}$$

The perturbed distribution can be expanded azimuthally,

$$\psi_1(r,\phi;s) = \sum_m \alpha_m R_m(r) e^{im\phi - i\Omega s/v} \ , \tag{9.6}$$

where $R_m(r)$ are functions corresponding to the mth azimuthal, α_m are the expansion coefficients, and $\Omega/(2\pi)$ is the collective frequency to be determined. The Vlasov equation becomes

$$(\Omega - m\omega_s)\alpha_m R_m(r) e^{-i\Omega s/v} = -\frac{iv\eta}{E_0\omega_s\beta^2}\frac{d\psi_0}{dr}\int_{-\pi}^{\pi}\frac{d\phi}{2\pi}\, e^{-im\phi}\sin\phi\,\langle F_0^{\parallel}(\tau;s)\rangle \ . \tag{9.7}$$

Now consider the wake force acting on a beam particle at location s, where a cavity gap is located for example, with time advance τ relative to the synchronous particle due to all preceding particles passing through s at an earlier time. This force can be expressed as

$$\langle F_0^{\parallel}(\tau;s)\rangle = -\frac{e^2}{C}\sum_{k=-\infty}^{\infty}\int_{-\infty}^{\infty} d\tau' \rho_1[\tau', s-kC-v(\tau'-\tau)]W_0'[kC+v(\tau'-\tau)] \ , \qquad (9.8)$$

where only the perturbed density ρ_1, which is the projection of ψ_1 onto the τ axis, is included, because the unperturbed part should have been considered in the zeroth order of the Vlasov equation during the discussion of potential-well distortion. The summation over k takes care of the contribution of the wake left by the charge distribution in previous turns. The lower limit of the summation and the lower limit of the integral have been extended to $-\infty$ because of the causality property of the wake function. The expression in Eq. (9.8) is more accurate than the on in Eq. (2.7). In the latter, we assume the particle density does not change from the time the source particles pass the reference point to the time when the test particle observes the wake at the same reference point. Such an assumption is no longer valid here because the wake is left by particles in other bunches which may be many revolution turns ahead and these bunches are oscillating azimuthally in the longitudinal phase space. When the source particle, with time advance τ' with reference to the synchronous particle and k turns ahead of the test particle, is at location s to excite the cavity, the test particle is at location $s-kC-v(\tau'-\tau)$. Hence, we have the second argument in the perturbation linear density ρ_1.

There are M bunches and the synchronous particle in the ℓth bunch is at location s_ℓ. If the witness particle is in the nth bunch,

$$\langle F_{0n}^{\parallel}(\tau;s)\rangle = -\frac{e^2}{C}\sum_{k=-\infty}^{\infty}\sum_{\ell=0}^{M-1}\int_{-\infty}^{\infty} d\tau' \times$$
$$\times\, \rho_\ell\big[\tau'; s-kC-(s_\ell-s_n)-v(\tau'-\tau)\big]W_0'\big[kC+(s_\ell-s_n)+v(\tau'-\tau)\big] \ . \qquad (9.9)$$

We assume the bunches are identical and equally spaced. For the μth coupled mode, we substitute in the above expression the perturbed density of the nth bunch $\rho_{1n}(\tau)e^{-i\Omega s/v}$ including the phase lead,

$$\rho_\ell(\tau;s) = \rho_{1n}(\tau)e^{i2\pi\mu(\ell-n)/M}e^{-i\Omega s/v} \ . \qquad (9.10)$$

Next, let us go to the frequency domain using the Fourier transforms

$$W_0'(v\tau) = \frac{1}{2\pi}\int_{-\infty}^{\infty} d\omega\, Z_0^{\parallel}(\omega)e^{-i\omega\tau} \ , \qquad (9.11)$$

$$\rho_{1n}(\tau) = \int_{-\infty}^{\infty} d\omega\, \tilde{\rho}_{1n}(\omega) e^{i\omega\tau} \ . \tag{9.12}$$

In Eq. (9.9) above, we shall neglect[‡] the time delay $\tau' - \tau$ in ρ_ℓ because this will only amount to a phase delay $\Omega(\tau' - \tau)$ where $\Omega \approx m\omega_s$, which is very much less than the phase change $\omega_r(\tau' - \tau)$ during the bunch passage, where $\omega_r/(2\pi)$ is the frequency of the driving resonant impedance. Substituting Eqs. (9.11) and (9.12) into Eq. (9.9) and integrating over τ' and one of the ω's, the wake force for the μth coupled-bunch mode becomes

$$\begin{aligned}\langle F^{\parallel}_{0n\mu}(\tau; s)\rangle = -\frac{e^2}{C} \sum_{k=-\infty}^{\infty} \sum_{\ell=0}^{M-1} e^{i2\pi\mu(\ell-n)/M} e^{i\Omega(-s+kC+s_\ell-s_n)/v} \times \\ \times \int_{-\infty}^{\infty} d\omega \tilde{\rho}_{1n}(\omega) Z_0^{\parallel}(\omega) e^{-i\omega(kC+s_\ell-s_n)/v} e^{i\omega\tau} \ .\end{aligned} \tag{9.13}$$

The summation over k can now be performed using Poisson formula

$$\sum_k e^{-ik\omega C/v} = \sum_p 2\pi\, \delta\left(\frac{\omega C}{v} - 2\pi p\right) = \sum_p \omega_0\, \delta(\omega - p\omega_0) \ . \tag{9.14}$$

This leads to

$$\langle F^{\parallel}_{0n\mu}(\tau; s)\rangle = -\frac{e^2}{C} \sum_{p=-\infty}^{\infty} \sum_{\ell=0}^{M-1} e^{i2\pi\mu(\ell-n)/M} e^{-i\Omega s/v + i\omega_p\tau} \omega_0 \tilde{\rho}_{1n}(\omega_p) Z_0^{\parallel}(\omega_p) e^{-ip\omega_0(s_\ell - s_n)/v} \ , \tag{9.15}$$

where we have used the short-hand notation

$$\omega_p = p\omega_0 + \Omega \ . \tag{9.16}$$

We next make use of the fact that the unperturbed bunches are equally spaced, or

$$s_\ell - s_n = \frac{\ell - n}{M} C \ . \tag{9.17}$$

The summation over ℓ can be performed. The sum vanishes unless $(p-\mu)/M = q$, where q is an integer:

$$\sum_{\ell=0}^{M-1} e^{i2\pi(\ell-n)(\mu-p)/M} = \begin{cases} M & \text{if } \dfrac{p-\mu}{M} = q\,, \\ 0 & \text{otherwise}\,. \end{cases} \tag{9.18}$$

[‡]Without this approximation, only $Z_0^{\parallel}$ will have the argument ω_p in Eq. (9.15). The argument of $\tilde{\rho}$ and the factor in front of τ in the exponent will be replaced by $\omega_p - \Omega$. In Eq. (9.19) below, The argument of $\tilde{\rho}$ and the factor in front of τ in the exponent will be replaced by $\omega_q - \Omega$.

The final result is

$$\langle F^{\|}_{0n\mu}(\tau;s)\rangle = -\frac{e^2 M\omega_0}{C}\, e^{-i\Omega s/v} \sum_{q=-\infty}^{\infty} \tilde{\rho}_{1n}(\omega_q) Z_0^{\|}(\omega_q) e^{i\omega_q \tau} \ , \tag{9.19}$$

where

$$\omega_q = (qM+\mu)\omega_0 + \Omega \ . \tag{9.20}$$

Since the left side of the Vlasov equation is expressed in terms of the radial function $R_m(r)$, we want to do the same for the wake force. First, rewrite the perturbed density in the time domain,

$$\langle F^{\|}_{0n\mu}(\tau;s)\rangle = -\frac{e^2 M\omega_0}{C}\, e^{-i\Omega s/v} \sum_{q=-\infty}^{\infty} Z_0^{\|}(\omega_q) \int \frac{d\tau'}{2\pi}\, \rho_{1n}(\tau') e^{i\omega_q(\tau-\tau')} \ . \tag{9.21}$$

Since $\rho_{1n}(\tau')$ is the projection of the perturbed distribution onto the τ' axis, we must have

$$\rho_{1n}(\tau')d\tau' = \int \psi_{1n}(\tau', \Delta E') d\tau' d\Delta E' \tag{9.22}$$

$$= \frac{E_0\omega_s\beta^2}{\eta} \int \psi_{1n}(r', \phi') r' dr' d\phi' \tag{9.23}$$

$$= \frac{E_0\omega_s\beta^2}{\eta} \sum_{m'} \alpha_{m'} \int R_{m'}(r') e^{im'\phi'} r' dr' d\phi' \ . \tag{9.24}$$

The wake force then takes the form

$$\langle F^{\|}_{0n}(\tau;s)\rangle = -\frac{e^2\omega_0 M}{2\pi C}\frac{E_0\omega_s\beta^2}{\eta}\, e^{-i\Omega s/v} \sum_{q=-\infty}^{\infty}\sum_{m'} Z_0^{\|}(\omega_q) \int r' dr' d\phi' \alpha_{m'} R_{m'}(r') e^{im'\phi'} e^{i\omega_q(\tau-\tau')} \ , \tag{9.25}$$

This wake force is next substituted into the Vlasov equation (9.7). The integrations over ϕ and ϕ' are performed in terms of Bessel function of order m using its integral definition

$$i^m J_m(z) = \frac{1}{2\pi}\int_{-\pi}^{\pi} d\phi\, e^{\pm im\phi + iz\cos\phi} \ , \tag{9.26}$$

the recurrence relation

$$J_{m-1}(z) + J_{m+1}(z) = \frac{2m}{z} J_m(z) \ , \tag{9.27}$$

and the fact that

$$J_m(-z) = (-1)^m J_m(z) \ . \tag{9.28}$$

The result is the Sacherer's integral equation for longitudinal instability for the mth azimuthal μth coupled-bunch mode,

$$(\Omega - m\omega_s)\alpha_m R_m(r) =$$
$$-\frac{i2\pi e^2 MN\eta}{\beta^2 E_0 T_0^2 \omega_s}\frac{m}{r}\frac{dg_0}{dr}\sum_{m'} i^{m-m'}\alpha_{m'}\int r'dr' R_{m'}(r')\sum_q \frac{Z_0^{\|}(\omega_q)}{\omega_q}J_{m'}(\omega_q r')J_m(\omega_q r)\,, \quad (9.29)$$

where transformation of the unperturbed longitudinal distribution

$$\psi_0(r)d\tau d\Delta E = \frac{\omega_s\beta^2 E_0}{\eta}\psi_0 dxdp_x = Ng_0(r)rdrd\phi \quad (9.30)$$

has been made so that g_0 is normalized to unity when integrated over $rdrd\phi$.

This is an eigenfunction-eigenvalue problem, the α_m's being the eigenfunctions and Ω the corresponding eigenvalue. The solution is nontrivial. However, with some approximations, interesting results can be deduced. When the perturbation is not too strong so that the shift in frequency is much less than the synchrotron frequency, there will not be coupling between different azimuthals. The integral equation simplifies to

$$(\Omega - m\omega_s)R_m(r) = -\frac{i2\pi e^2 MN\eta}{\beta^2 E_0 T_0^2 \omega_s}\frac{m}{r}\frac{dg_0}{dr}\int r'dr' R_m(r')\sum_q \frac{Z_0^{\|}(\omega_q)}{\omega_q}J_m(\omega_q r')J_m(\omega_q r)\,. \quad (9.31)$$

The spread in synchrotron frequency can be introduced by letting ω_s be a function of r. Moving the factor $\Omega - m\omega_s(r)$ to the right side, the radial distribution R_m can be eliminated by multiplying both sides by $rJ_m(r)$ and integrating over dr. We then arrive at the dispersion relation,

$$1 = -\frac{i2\pi e^2 MNm\eta}{\beta^2 E_0 T_0^2 \omega_s}\sum_q \frac{Z_0^{\|}(\omega_q)}{\omega_q}\int dr\,\frac{dg_0}{dr}\frac{J_m^2(\omega_q r)}{\Omega - m\omega_s(r)}\,. \quad (9.32)$$

Stability and growth contours can be derived from the dispersion relation of Eq. (9.32) in just the same way as in the discussion of microwave instability for a single bunch in Chapter 6.

9.1.1 Synchrotron Tune Shift

When the spread in synchrotron frequency is small, Eq. (9.32) gives the frequency shift

$$\Omega - m\omega_s = \frac{i2\pi e^2 MNm\eta}{\beta^2 E_0 T_0^2 \omega_s}\sum_q \frac{Z_0^{\|}(\omega_q)}{\omega_q}\left[-\int dr\,\frac{dg_0}{dr}J_m^2(\omega_q r)\right]\,, \quad (9.33)$$

where the expression inside the square brackets, denote by F, can be viewed as a distribution dependent form factor, which is positive definite because dg_0/dr is negative. The real part $\mathcal{R}e(\Omega - \omega_s)$ gives the coherent tune shift of the bunch while the imaginary part $\mathcal{I}m\,\Omega$ gives the growth rate of the instability.

When the bunch length $2\hat{\tau}$ is much shorter than the wavelength of the perturbing impedance, or $\omega_q\hat{\tau} \ll 1$, the Bessel function can be substituted by its small-argument expression:

$$J_m(x) \approx \frac{1}{m!}\left(\frac{x}{2}\right)^m \ . \tag{9.34}$$

We are interested in particular the synchrotron tune shift of one bunch ($M = 1$) in dipole mode ($m = 1$), and obtain

$$\Delta\Omega = -\frac{e^2 N\eta}{2\beta^2 E_0 T_0^2 \omega_s}\sum_q \omega_q\, \mathcal{I}m\, Z_0^{\parallel}(\omega_q) \ , \tag{9.35}$$

where $\omega_q = q\omega_0 + \omega_s$ and the bunch density normalization

$$\int g_0(r) r dr d\phi = 1 \tag{9.36}$$

has been used. In the situation that the perturbing impedance is a broadband resonance, we can make the approximation $\omega_q = q\omega_0$.

It is important to point out that Eq. (9.35) is only the dynamic part of the synchrotron tune shift contributed by the impedance. There is another contribution coming from the static potential-well distortion. This term is not present in Eq. (9.35), because during the derivation of the Sacherer's growth formula, we have substituted only the perturbed distribution into the wake force in Eq. (9.8) but not the unperturbed distribution. As a result, the static potential-well distortion piece has been left out. This static contribution has been addressed in Eq. (3.50). When the short bunch approximation is made, it can be shown that the static contribution just cancels the dynamic contribution, resulting in no coherent shift for the dipole mode (Exercise 9.2). This is evident physically because the dipole motion is rigid. The whole bunch moves as a whole, and therefore the bunch center does not experience any change in wake field from itself at all. On the other hand, an individual particle moving inside a bunch will experience the time variation of the wake left by the bunch and therefore the incoherent tune shift is nonzero.

9.1.2 Water Bag Model

Take the simple case of a single bunch of length $2\hat{\tau}$ and uniform distribution in the longitudinal phase space, which is usually called the *water bag model*. Then

$$g_0(r) = \frac{1}{\pi\hat{\tau}^2}\, H(\hat{\tau} - r) \ , \tag{9.37}$$

where the Heaviside function is defined as $H(x) = 1$ when $x > 0$ and zero otherwise. The form factor, the expression inside the square brackets of Eq. (9.33), becomes

$$F = \frac{1}{\pi\hat{\tau}^2}\, J_m^2(\omega_q\hat{\tau}) \approx \frac{\omega_q^2}{4\pi}\frac{1}{(m!)^2}\left(\frac{\omega_q\hat{\tau}}{2}\right)^{2m-2} \ , \tag{9.38}$$

where the assumption of a short bunch has been made in the last step. The growth rate driven by the impedance can now be written as

$$\frac{1}{\tau_m} = \frac{e^2 N\eta}{2\beta^2 E_0 T_0^2\omega_s}\frac{m}{(m!)^2}\sum_q \left(\frac{\omega_q\hat{\tau}}{2}\right)^{2m-2}\omega_q\, \mathcal{R}e\, Z_0^{\parallel}(\omega_q) \ , \tag{9.39}$$

where, for one bunch, $\omega_q = q\omega_0 + \Omega$.

9.1.3 Robinson's Instability

The $m = 0$ mode is a trivial mode which gives $\Omega_0 = 0$. It describes the potential-well distortion mode addressed in Chapter 3 and is of not much interest here where the emphasis is on instabilities. The next azimuthal mode is $m = 1$ which describes dipole oscillations and we expect $\Omega_1 \approx \omega_s$. Consider the situation of having the driving impedance as a resonance so narrow that there is only one $q > 0$ that satisfies

$$\omega_r \approx q\omega_0 \pm \omega_s \ , \tag{9.40}$$

where $\omega_r/(2\pi)$ is the resonant frequency. The growth rate for a short bunch can therefore be obtained from Eq. (9.39),

$$\frac{1}{\tau_1} = \mathcal{I}m\,\Delta\omega_s = \frac{\eta e^2 N\omega_r}{2\beta^2 E_0 T_0^2\omega_s}[\mathcal{R}e\, Z_0^{\parallel}(q\omega_0+\omega_s) - \mathcal{R}e\, Z_0^{\parallel}(q\omega_0-\omega_s)] \ , \tag{9.41}$$

where the first term corresponds to positive frequency and the second negative frequency. If the resonant frequency is slightly above $q\omega_0$ as illustrated in Fig. 9.1(a), we have

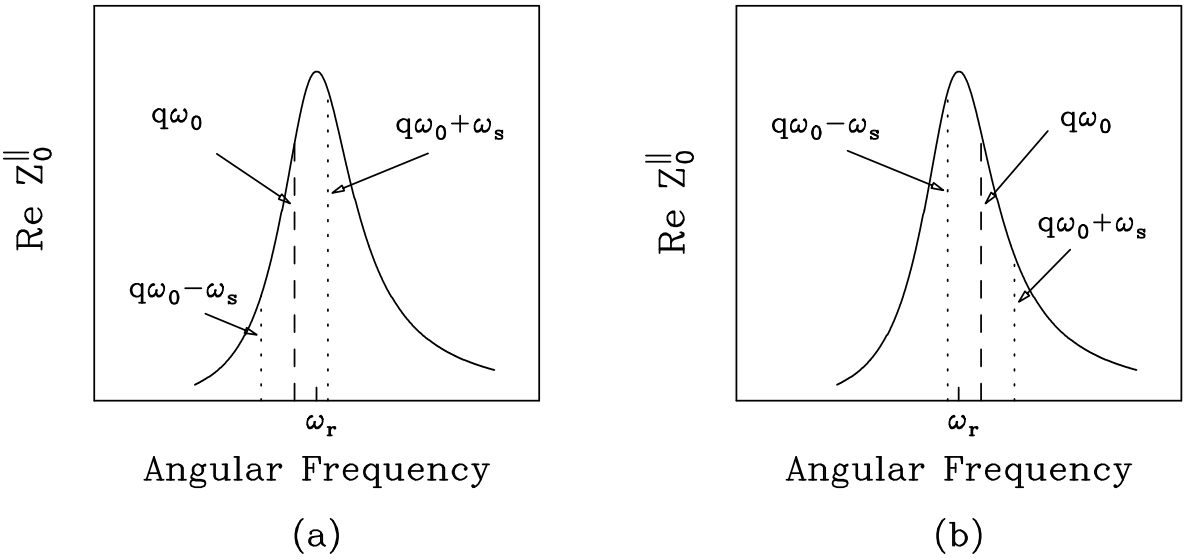

Figure 9.1: (a) Above transition, if the resonant frequency ω_r is slightly above a revolution harmonic $q\omega_0$, $\mathcal{R}e\, Z_0^{\parallel}$ at the upper synchrotron sideband is larger than at the lower synchrotron sideband. The system is unstable. (b) Above transition, if ω_r is slightly below a harmonic line, $\mathcal{R}e\, Z_0^{\parallel}$ at the upper sideband is smaller than at the lower sideband. The system is stable.

$\mathcal{R}e\, Z_0^{\parallel}(q\omega_0 + \omega_s) > \mathcal{R}e\, Z_0^{\parallel}(q\omega_0 - \omega_s)$. Above transition, the growth rate will be positive or there is instability. On the other hand, if $\omega_r < q\omega_0$ as illustrated in Fig. 9.1(b), the growth rate is negative and the system is damped. This instability criterion was first analyzed by Robinson [1], and we have obtained exactly the same result in Sec. 8.3.3 using phasor diagram analysis. Below transition, the inverse is true; one should tune the resonant frequency of the cavity below a revolution harmonic for stability. Note that the growth rate of Eq. (9.41) is independent of the bunch length when the bunch is short, implying that for the dipole mode, this is a point-bunch theory.[§] Thus, this special case should be obtainable much more easily than the complicated derivation that we have gone through, and it is worthwhile to make a digression into this easier derivation.

9.1.3.1 Point-Bunch Theory

Let us start from the equations of motion of a super particle with arrival time advance $\tau(s)$, carrying charge eN, and seeing its own wake left behind k revolutions before. We

[§]More about Robinson's stability criterion was discussed in Chapter 7.5.

have

$$\frac{d^2\tau}{ds^2} + \frac{\omega_s^2}{v^2}\,\tau = \frac{e^2 N\eta}{v\beta^2 E_0 C}\sum_{k=-\infty}^{\infty} W_0'\left[kT_0 + \tau(s-kC) - \tau(s)\right] \ , \tag{9.42}$$

where the summation has been extended to $-\infty$ (the future) because the wake function obeys causality. The arrival time advance of each passage through the cavity gap is of the order of the synchrotron oscillation amplitude, which should be small. We can therefore expand the wake potential about kT_0. The right side becomes

$$\begin{aligned} \text{R.S.} &= \frac{e^2 N\eta}{v\beta^2 E_0 C}\sum_{k=-\infty}^{\infty}\left[\tau(s-kC) - \tau(s)\right] W_0''(kT_0) \\ &= \frac{e^2 N\eta}{v\beta^2 E_0 C}\,\tau(s)\sum_{k=-\infty}^{\infty}\left[e^{-i\Omega(s/v - kT_0)} - 1\right] W_0''(kT_0) \ , \end{aligned} \tag{9.43}$$

where we have substituted the collective time behavior

$$\tau(s) \propto e^{-i\Omega s/v} \ , \tag{9.44}$$

with Ω being the collective angular frequency to be determined. Next go to the frequency domain by introducing the longitudinal impedance $Z_0^{\|}$, or

$$W_0'(t) = \frac{1}{2\pi}\int d\omega Z_0^{\|}(\omega) e^{-i\omega t} \ . \tag{9.45}$$

We obtain

$$\text{R.S.} = -\frac{ie^2 N\eta}{v\beta^2 E_0 C}\sum_{k=-\infty}^{\infty}\left[e^{-i\Omega(s/v - kT_0)} - 1\right]\int \frac{d\omega}{2\pi}\,\omega Z_0^{\|}(\omega) e^{-i\omega kT_0} \ . \tag{9.46}$$

The summation over k can now be performed. Substituting the time behavior of τ into the left side, the equation of motion becomes

$$\Omega^2 - \omega_s^2 = \frac{ie^2 N\eta v^2}{\beta^2 E_0 C^2}\sum_{p=-\infty}^{\infty}\left[(p\omega_0 + \Omega) Z_0^{\|}(p\omega_0 + \Omega) - p\omega_0 Z_0^{\|}(p\omega_0)\right] \ . \tag{9.47}$$

Finally, assuming that the perturbation is small, the result simplifies to

$$\Delta\Omega = \frac{ie^2 N\eta}{2\beta^2 E_0 T_0^2 \omega_s}\sum_{p=-\infty}^{\infty}\left[(p\omega_0 + \omega_s) Z_0^{\|}(p\omega_0 + \omega_s) - p\omega_0 Z_0^{\|}(p\omega_0)\right] \ . \tag{9.48}$$

The above shift in synchrotron frequency gives exactly the same growth rate as Eq. (9.41) when the driving impedance is a narrow resonance. The only difference is the second

term in Eq. (9.48). This term receives contribution from the imaginary part of the impedance only and describes the tune shift due to potential-well distortion. The origin of this term is very similar to the derivation of Eqs. (3.50) and (3.51). The only thing additional here is the inclusion of the wake effect from preceding bunch passages. Here, the wake field from preceding bunch passages does not move with the bunch as a whole, and therefore contributes a viewable coherent tune shift. This term should also appear in the Sacherer's growth formula. It has been left out because, during the derivation, only the perturbed distribution but not the unperturbed distribution have been substituted into the wake force in Eq. (9.8).

Now let us come back to Eq. (9.41). For M equal bunches, the equation becomes, for coupled-bunch mode μ,

$$\frac{1}{\tau_{1\mu}} = \frac{\eta e^2 N M \omega_r}{2\beta^2 E_0 T_0^2 \omega_s} \left[\mathcal{R}e\, Z_0^{\parallel}(qM\omega_0 + \mu\omega_0 + \omega_s) - \mathcal{R}e\, Z_0^{\parallel}(q'M\omega_0 - \mu\omega_0 - \omega_s) \right] . \qquad (9.49)$$

When $\mu = 0$, both terms will contribute with $q' = q$ and we have exactly the same Robinson's stability or instability as in the single bunch situation. This is illustrated in Fig. 9.2. When $\mu = M/2$ if M is even, both terms will contribute with $q' = q$, and the same Robinson's stability or instability will apply. For the other $M-2$ modes, only one term will be at or close to the resonant frequency and only one term will contribute. If the positive-frequency term contributes, we have instability. If the negative-frequency term contributes, we have damping instead. If one choose to speak in the language of only positive frequencies, there will be an upper and a lower synchrotron sideband surrounding each revolution harmonic. Above transition, the coupled-bunch system will be unstable if the driving resonance leans towards the upper sideband and stable if it leans towards the lower sideband.

For the higher azimuthal modes ($m > 1$) driven by a narrow resonance, we have the same Robinson's instability. The growth rates are

$$\begin{aligned} \frac{1}{\tau_{m\mu}} =& \frac{\eta e^2 N M \omega_r}{2\beta^2 E_0 T_0^2 \omega_s} \frac{m}{(m!)^2} \left(\frac{\omega_r \hat{\tau}}{2} \right)^{2m-2} \times \\ & \times \left[\mathcal{R}e\, Z_0^{\parallel}(qM\omega_0 + \mu\omega_0 + m\omega_s) - \mathcal{R}e\, Z_0^{\parallel}(q'M\omega_0 - \mu\omega_0 - m\omega_s) \right] , \end{aligned} \qquad (9.50)$$

which depend on the bunch length as $\hat{\tau}^{2m-2}$. As a result, higher azimuthal instabilities for short bunches will be much more difficult to excite. For long bunches, we need to evaluate the form factor F. An example will be discussed in Sec. 9.2.

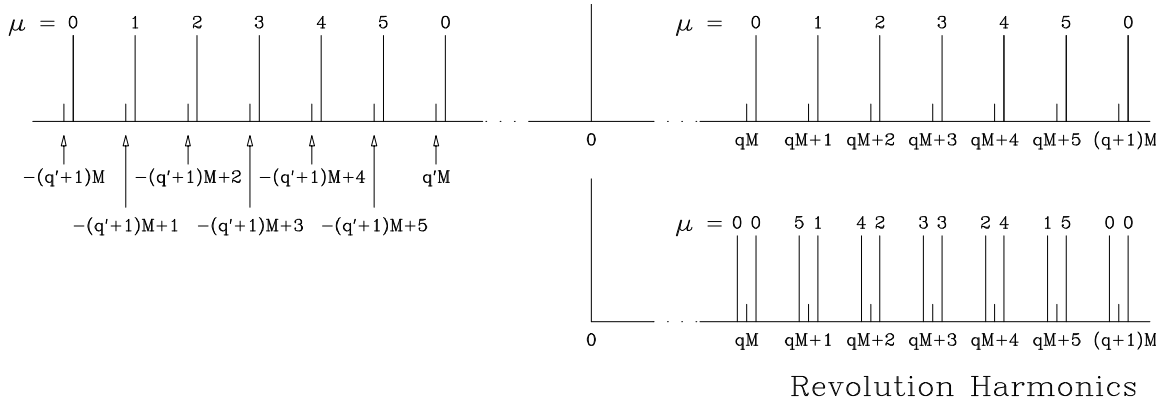

Figure 9.2: Top plot shows the synchrotron lines for both positive and negative revolution harmonics for the situation of $M = 6$ identical equally-spaced bunches. The coupled-bunch modes $\mu = 0, 1, 2, 3, 4, 5$ are listed at the top of the synchrotron lines. Lower plot shows the negative-harmonic side folded onto the positive-harmonic side. We see upper and lower sidebands for each harmonic line.

Landau damping can come from the spread of the synchrotron frequency. The spread due to the nonlinear sinusoidal rf wave form can be written as (Exercise 9.4)

$$\frac{\Delta\omega_s}{\omega_s} = \left(\frac{\pi^2}{16}\right)\left(\frac{1+\sin^2\phi_s}{1-\sin^2\phi_s}\right)(h\tau_L f_0)^2 \ , \tag{9.51}$$

where τ_L is the total length of the bunch and ϕ_s is the synchronous angle, and is valid for small amplitudes. The mode will be stable if [2]

$$\frac{1}{\tau} \lesssim \frac{\sqrt{m}}{4}\Delta\omega_s \ . \tag{9.52}$$

When the synchronous angle $\phi_s \neq 0$, the computation of synchrotron frequency spread is tedious. A numerical calculation is shown in Fig. 9.3 for various $\Gamma = \sin\phi_s$. The expression in Eq. (9.51) comes from a fitting to the numerical calculation at small amplitudes.

9.2 Time Domain

The longitudinal coupled-bunch instabilities can also be studied without going into the frequency domain. We are employing the same Vlasov equation in Eq. (9.7), but using

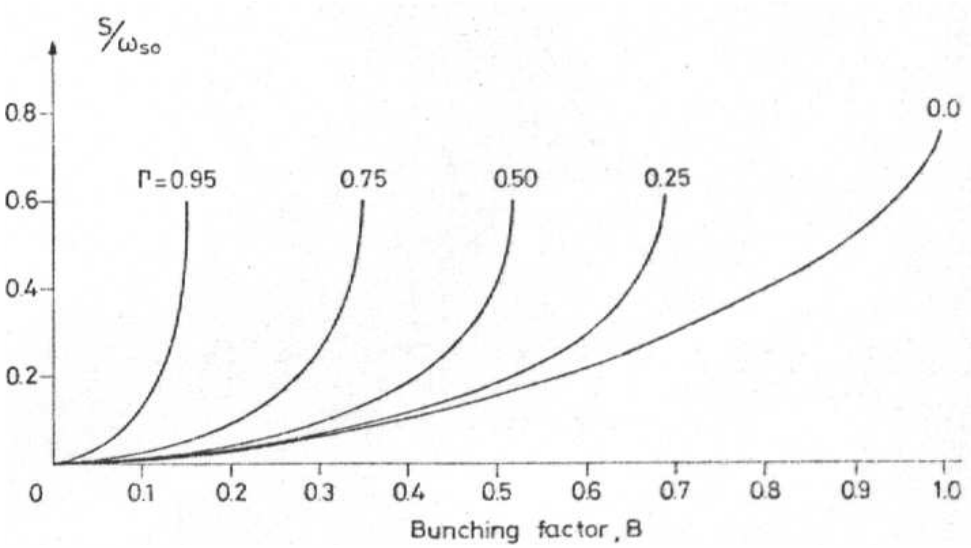

Figure 9.3: Synchrotron frequency spread S as a function of single-bucket bunching factor $B \approx \tau_L f_0$ for various values of $\Gamma = \sin\phi_s$. τ_L is full bunch length, f_0 is revolution frequency, ϕ_s is synchronous angle, and ω_{s0} is unperturbed angular synchrotron frequency.

the wake function of a resonance in the time domain. This derivation was first given by Sacherer [2].

The wake function for a resonance with resonant frequency $\omega_r/(2\pi)$, shunt impedance R_s and quality factor Q was given in Eq. (1.46). For a narrow resonance with $\alpha = \omega_r/(2Q) \ll \omega_r$, we can neglect the sine term[¶] and simplify the wake function to

$$W_0'(z) = \frac{\omega_r R_s}{Q}\, e^{-\alpha z/v} \cos\frac{\omega_r z}{v} \qquad \text{when } z > 0\ . \tag{9.53}$$

The wake force is then given by

$$\langle F_0^{\parallel}(\tau; s)\rangle = -\frac{e^2\omega_r R_s}{QC}\int_\tau^\infty d\tau'\, e^{-\alpha(\tau'-\tau)} \cos[\omega_r(\tau'-\tau)]\, \rho\,[\tau'; s - v(\tau'-\tau)]\ , \tag{9.54}$$

where $\rho\,[\tau'; s - v(\tau'-\tau)]$ is the linear density of the beam particles passing the location s at time $\tau' - \tau$ ago. Now let $\rho(\tau; s)$ represent the line density of the individual bunch, which has a phase lead of $2\pi\mu/M$ for mode μ compared with the preceding bunch $\tau_{\text{sep}} = T_0/M$ ahead, and is influenced by all the preceding bunches. The location argument s

[¶]The sine term can be included at the expense of a slightly more complicated derivation.

of ρ in Eq. (9.54) becomes[‖] $s - k\tau_{\rm sep} - v(\tau' - \tau)$, with $k = 0,\ 1,\ 2,\ \cdots$. For simplicity, we neglect the time delay $\tau' - \tau$. In the time variation $e^{-i\Omega s/v}$ where $\Omega \approx m\omega_s$, this approximation causes a phase delay $\Omega(\tau' - \tau)$ which is negligible in comparison with the phase change due to the resonator. We will also neglect the variation in the attenuation factor over one bunch $e^{-\alpha(\tau' - \tau)}$, but we retain the attenuation factor between bunches $e^{-\alpha k \tau_{\rm sep}}$. Then the wake force exerted on a particle in the μth coupled-bunch mode can be written as

$$\langle F^{\|}_{0\mu}(\tau; s)\rangle = -\frac{e^2\omega_r R_s}{QC}\sum_{k=0}^{\infty} e^{2\pi i k\mu/M - k\alpha\tau_{\rm sep}} \int_{\substack{\rm one\\ \rm bunch}} d\tau' \cos[\omega_r(\tau' - \tau + k\tau_{\rm sep})]\, \rho_1(\tau') e^{-i\Omega(s/v - k\tau_{\rm sep})}\,, \tag{9.55}$$

where Eq. (9.10), the 'time' variations of preceding bunches in the μth coupled mode, have been used. It is worth pointing out that the lower limits of the summation and integration *cannot* be extended to $-\infty$ as before, because the explicit expression of the wake function has been used. Note that only the perturbed line density ρ_1 is included. This is because we are interested in the growth rate here and the unperturbed part ρ_0 will not contribute to the growth rate. Changing the integration variables from $(\tau, \Delta E)$ to (r, ϕ) while keeping only the azimuthal m,

$$\rho_1(\tau')d\tau' = \int \alpha_m R_m(r') e^{im\phi'} d\tau' d\Delta E' = \int \frac{E_0\omega_s\beta^2}{\eta}\, \alpha_m R_m(r') e^{im\phi'} r' dr' d\phi' \ . \tag{9.56}$$

Substituting the wake force into Eq. (9.7), we arrive at

$$\begin{aligned}(\Omega - m\omega_s) R_m(r) = {} & \frac{ie^2 N\eta\omega_r R_s}{2\pi\beta^2 E_0 Q T_0 \omega_s}\frac{dg_0}{dr}\sum_{k=0}^{\infty} e^{2\pi i k\mu/M - k(\alpha - i\Omega)\tau_{\rm sep}} \times \\ & \times \int_0^{\infty} r' dr' R_m(r') \int_{-\pi}^{\pi} d\phi\, e^{-im\phi} \sin\phi \int_{-\pi}^{\pi} d\phi' e^{im\phi'} \cos[\omega_r(r'\cos\phi' - r\cos\phi + k\tau_{\rm sep})]\,, \end{aligned} \tag{9.57}$$

where again we have used the unperturbed distribution $g_0(r)$ given by Eq.(9.30) which is normalized to unity. The integrations over ϕ and ϕ' can now be performed using the formulas for Bessel functions depicted in Eqs. (9.26) to (9.28), giving

$$\begin{aligned}\int_{-\pi}^{\pi} d\phi\, e^{-im\phi} \sin\phi \int_{-\pi}^{\pi} d\phi' e^{im\phi'} \cos[\omega_r(r'\cos\phi' - r\cos\phi + k\tau_{\rm sep})] = {} & \\ i4\pi^2 \sin k\omega_r\tau_{\rm sep}\, \frac{m J_m(\omega_r r') J_m(\omega_r r)}{\omega_r r}\ . & \end{aligned} \tag{9.58}$$

[‖]Here we include the term $k\tau_{\rm sep}$ which Sacherer had left out. This term is important to exhibit Robinson's criterion of phase stability.

Equation (9.57) now becomes

$$(\Omega - m\omega_s)R_m(r) = -\frac{2\pi e^2 N R_s m\eta}{\beta^2 E_0 Q T_0 \omega_s}\frac{dg_0}{dr}\times$$
$$\times \sum_{k=0}^{\infty} e^{2\pi i k\mu/M - k(\alpha - i\Omega)\tau_{\rm sep}} \sin(k\omega_r\tau_{\rm sep}) \int_0^\infty dr' R_m(r') \frac{r' J_m(\omega_r r') J_m(\omega_r r)}{r} . \quad (9.59)$$

Finally, we introduce Landau damping by allowing the synchrotron frequency to be a function of the radial distance from the center of the bunch in the longitudinal phase space. Moving $\Omega - m\omega_s(r)$ to the right side and performing an integration over rdr, R_m can be eliminated resulting in the dispersion relation

$$1 = -\frac{i2\pi e^2 M N m\eta R_s}{\beta^2 E_0 T_0^2 \omega_s \omega_r} D(\alpha\tau_{\rm sep}) \int_0^\infty dr \frac{dg_0}{dr} \frac{J_m^2(\omega_r r)}{\Omega - m\omega_s(r)} , \quad (9.60)$$

where we have defined the function**

$$D(\alpha\tau_{\rm sep}) = -i2\alpha\tau_{\rm sep} \sum_{k=0}^{\infty} e^{2\pi i k\mu/M - k(\alpha - i\Omega)\tau_{\rm sep}} \sin(k\omega_r\tau_{\rm sep}) , \quad (9.61)$$

which contains all the information about the quality factor of the resonance and its location with respect to the revolution harmonics. It is interesting to note that Eq. (9.60) closely resembles Eq. (9.32). It will be shown below that $D = 1$ for a narrow resonance with the resonant peak located at $(qM+\mu)\omega_0 + m\omega_s$. Thus the two dispersion relations are identical. In fact, they are the same even when the resonant peak is not exactly located at a synchrotron line.

Let us study the function $D(\alpha\tau_{\rm sep})$. Noting that the bunch separation is $\tau_{\rm sep} = T_0/M$, this function can be rewritten as

$$D(\alpha\tau_{\rm sep}) = \alpha\tau_{\rm sep}\left(\frac{1}{1-e^{x_+}} - \frac{1}{1-e^{x_-}}\right) , \quad (9.62)$$

where

$$x_\pm = \frac{2\pi i}{M}\left(q_\pm M + \mu + m\frac{\omega_s}{\omega_0} \mp \frac{\omega_r}{\omega_0}\right) - \alpha\tau_{\rm sep} . \quad (9.63)$$

The $q_\pm M$ term comes about because we can replace μ in Eq. (9.61) by $q_\pm M+\mu$, where $q_\pm$ are positive/negative integers and $\mu = 0,\ 1,\ \cdots,\ M-1$. When the resonance is

**We would like $D = \pm 1$ when the resonance is at the upper/lower sideband. As a result, our definition of D differs from Sacherer's by a phase.

extremely narrow, we have $\alpha\tau_{\rm sep} = \omega_r\tau_{\rm sep}/(2Q) \ll 1$. The two terms in Eq. (9.62) almost cancel each other so that $D(\alpha\tau_{\rm sep}) \approx 0$ unless $\omega_r \approx (|q_\pm|M \pm \mu)\omega_0$. For modes $\mu \neq 0$ and $\mu \neq \frac{1}{2}M$ if M is even, only one of the two terms in Eq. (9.62) contributes. If $\omega_r \approx (|q_\pm|M \pm \mu)\omega_0 \pm m\omega_s$, we have $|x_+| \ll 1$ or $|x_-| \ll 1$ and

$$D(\alpha\tau_{\rm sep}) \approx \mp\frac{\alpha\tau_{\rm sep}}{x_\pm} = \frac{-i\omega_r/(2Q)}{\omega_r - [(|q_\pm|M \pm \mu)\omega_0 \pm m\omega_s] \mp i\omega_r/(2Q)} \approx \pm 1 \ . \tag{9.64}$$

When $\mu = 0$ or $\mu = M/2$ if M is even, it is possible to choose q_+ and q_- so that both terms will contribute. We have

$$D \approx \frac{-i\omega_r/(2Q)}{\omega_r - [(q_+M+\mu)\omega_0 + m\omega_s] - i\omega_r/(2Q)} + \frac{-i\omega_r/(2Q)}{\omega_r - [(|q_-|M-\mu)\omega_0 - m\omega_s] + i\omega_r/(2Q)} \ , \tag{9.65}$$

where $q_+ = |q_-|$ for $\mu = 0$ and $|q_-| = q_+ + 1$ for $\mu = M/2$. Note that Eq. (9.65) is just proportional to the difference between $Z_0^{\parallel}(q_+M\omega_0 + \mu\omega_0 + m\omega_s + i\alpha)$ and $Z_0^{\parallel}(|q_-|M\omega_0 - \mu\omega_0 - m\omega_s - i\alpha)$; the Robinson's stability criterion derived in Eq. (9.49) is therefore recovered.

On the other hand, when the resonance is broad, $\alpha\tau_{\rm sep} \gg 1$. The first few terms in Eq. (9.61) dominate. Since $k = 0$ does not contribute, we include here only the next term,

$$D(\alpha\tau_{\rm sep}) \approx -i2\alpha\tau_{\rm sep}\sin(\omega_r\tau_{\rm sep})e^{2\pi i\mu/M - \alpha\tau_{\rm sep}} \ . \tag{9.66}$$

The magnitude $|D|$ becomes mode independent and exhibits a maximum when $\omega_r\tau_{\rm sep} = 2\pi\left(q + \frac{1}{4}\right)$. Thus the coupled-bunch modes near $\mu = \pm\frac{1}{4}M$ are most strongly excited, although $|D|$ will be much less than unity. Figure 9.4 plots $|D|$ versus ω_r/ω_0 for the situation of $M = 10$ bunches. The solid vertical lines show $|D| \approx 1$ for narrow resonance. The dotted curve are for broadband resonance when the bunch-to-bunch attenuation decrement is $\alpha\tau_{\rm sep} = 4$; the values of $|D|$ are small and appear to be mode-independent. The dashed curves correspond the intermediate case with bunch-to-bunch attenuation decrement $\alpha\tau_{\rm sep} = 1$. From left to right, they are for modes $\mu = 0$, 1 and 9, 2 and 8, 3 and 7, 4 and 6, 5. We see that $|D|_{\rm max}$ is roughly the same for each mode. Note that $\alpha\tau_{\rm sep} = 1$ translates into $(\Delta\omega_r/\omega_0)_{\rm FWHM} = M/\pi = 3.2$ or the resonance covers more than 3 revolution harmonics. Apparently, the figure shows that no mode will be excited if the ω_r/ω_0 falls exactly on qM or $q(\frac{1}{2}M)$ if M is even. This incorrect result appears because in drawing the plot, the limit $\omega_s \to 0$ has been taken. Figure 9.5 plots $|D|_{\rm max}$ versus the bunch-to-bunch decrement $\alpha\tau_{\rm sep}$, showing that it is less than 5% from unity when $\alpha\tau_{\rm sep} < 0.55$.

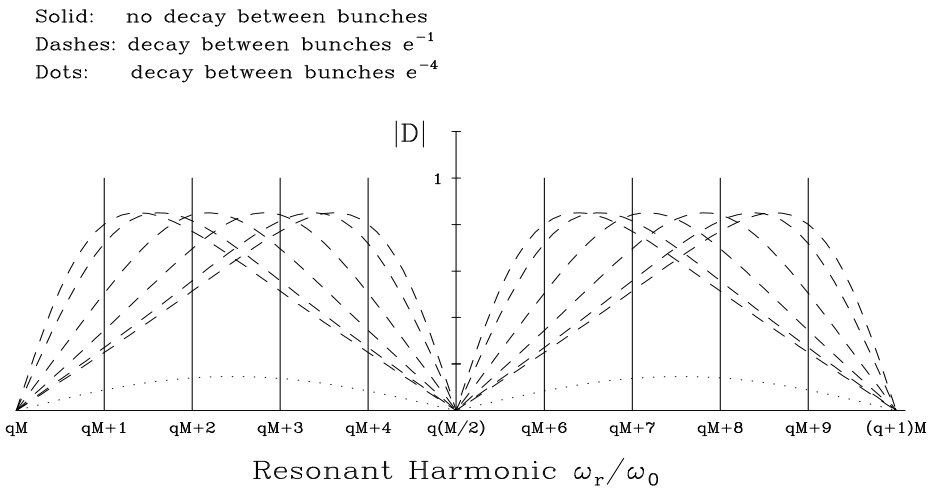

Figure 9.4: $|D|$ as functions of resonant harmonic ω_r/ω_0 for $M = 10$ bunches when bunch-to-bunch decay decrement $\alpha\tau_{\rm sep} \ll 1$ for narrowband resonance (solid), $\alpha\tau_{\rm sep} = 4$ for broadband resonance (dots), and $\alpha\tau_{\rm sep} = 1$ for resonance in between (dashes). The dashed curves from left to right represent coupled-bunch modes $\mu = 0$, 1 and 9, 2 and 8, 3 and 7, 4 and 6, 5. The excitations at $\omega_r/\omega_0 = 0$, or $M/2$ are zero, because we have set the synchrotron frequency to zero in the plot.

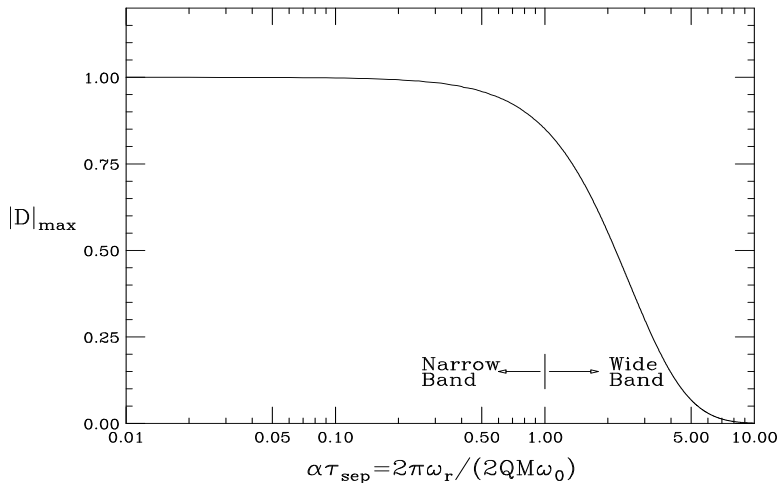

Figure 9.5: $|D|_{\rm max}$ as a function of bunch-to-bunch decay decrement $\alpha\tau_{\rm sep}$. Note that $|D|_{\rm max} \approx 1$ for narrow resonances but drops very rapidly as the resonance becomes broader.

In the event that the spread in synchrotron frequency is small, we can obtain from Eq. (9.60) the synchrotron frequency shift

$$\Omega - m\omega_s = -\frac{i2\pi e^2 N R_s m M \eta}{\beta^2 E_0 \omega_s \omega_r T_0^2} D(\alpha\tau_{\rm sep}) \int_0^\infty dr \frac{dg_0}{dr} J_m^2(\omega_r r) \ , \tag{9.67}$$

where the integral can be viewed as a form factor which is distribution dependent. A dimensionless form factor

$$F_m(\Delta\phi) = -\frac{4\pi m\hat{\tau}}{\omega_r} \int_0^\infty dr \frac{dg_0}{dr} J_m^2(\omega_r r) \tag{9.68}$$

can now be defined for each azimuthal, where $\hat{\tau}$ is the half bunch length and $\Delta\phi = 2\omega_r\hat{\tau}$ is the change in phase of the resonator during the passage of the whole bunch. Then the frequency shift can be rewritten as

$$\Omega - m\omega_s = \frac{i\eta e^2 N M R_s}{4\pi\beta^2 E_0 \nu_s T_0 \hat{\tau}} D(\alpha\tau_{\rm sep}) F_m(\Delta\phi) \ , \tag{9.69}$$

where $\nu_s = \omega_s/\omega_0$ is the synchrotron tune.

We take as an example the *parabolic* distribution in the longitudinal phase space[††], which implies

$$g_0(r) = \frac{2}{\pi\hat{\tau}^4}(\hat{\tau}^2 - r^2) \qquad \text{and} \qquad \frac{dg_0}{dr} = -\frac{4r}{\pi\hat{\tau}^4} \ . \tag{9.70}$$

The form factor is

$$\begin{aligned} F_m(\Delta\phi) &= \frac{32m}{\Delta\phi} \int_0^1 J_m^2(\tfrac{1}{2}x\Delta\phi) x dx \\ &= \frac{16m}{\Delta\phi}\Big[J_m^2\left(\tfrac{1}{2}\Delta\phi\right) - J_{m+1}\left(\tfrac{1}{2}\Delta\phi\right) J_{m-1}\left(\tfrac{1}{2}\Delta\phi\right)\Big] \ , \end{aligned} \tag{9.71}$$

which is plotted in Fig. 9.6 for $m = 1$ to 6. The form factor specifies the efficiency with which the resonator can drive a given mode. We see that the maximum value of F_1 for the dipole mode occurs when $\Delta\phi \approx \pi$. This is to be expected because the head and tail of the bunch will be driven in opposite directions. Similarly, the quadrupole or breathing mode is most efficiently driven when $\Delta\phi \approx 2\pi$, and so on for the higher modes. In general, mode m is most efficiently driven when the resonator frequency is $\Delta\phi \approx m\pi$. Note also that the maximum value of F_m drops faster than $m^{-1/2}$, implying that higher azimuthal modes are harder to excite. For distributions other than the "parabolic" of Eq. (9.70),

[††]This is different from the so-called parabolic distribution, which is actually parabolic line density.

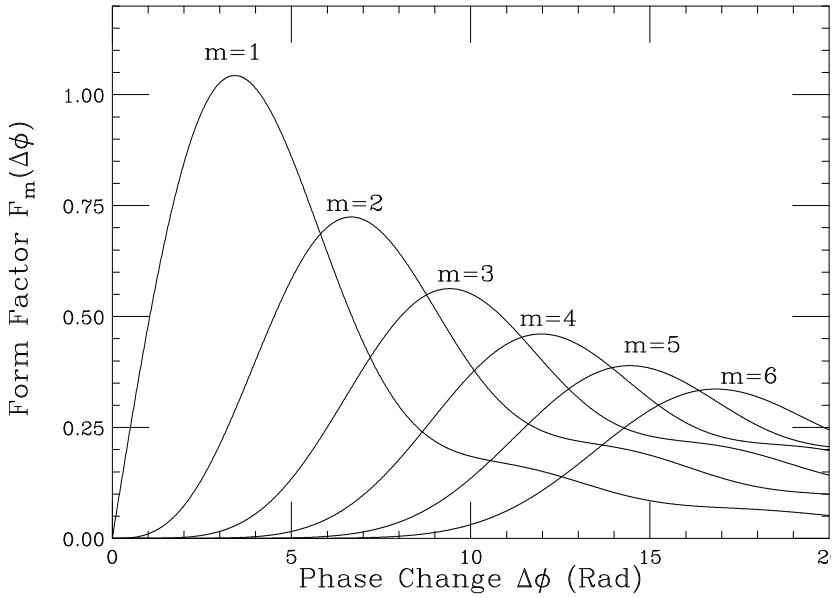

Figure 9.6: Sacherer's form factor for longitudinal oscillation inside a bunch with azimuthal modes $m = 1,\ 2,\ 3,\ 4,\ 5$ and 6. The unperturbed parabolic distribution in the longitudinal phase space, Eq. (9.70), is assumed.

we expect the form factors to have similar properties. However, a shorter bunch does not necessarily imply a slower growth especially for the $m = 1$ mode, although the excitation in the form factor $F_m(\Delta\phi)$ is small. According to Eq. (9.69), the growth rate is obtained from multiplying the form factor $F_m(\Delta\phi)$ with $eN/\hat{\tau}$, the local linear charge density or peak current. In fact, with a fixed number of particles in the bunch, as the bunch length is shortened, the local linear charge density increases, thus enhancing the growth rate. As a result, a more practical form factor should be $\bar{F}_m(\Delta\phi) = 2F_m(\Delta\phi)/\Delta\phi$ as plotted in Fig. 9.7 in logarithmic scale. It is clear that for small $\Delta\phi$, $F_1 \approx \frac{1}{2}\Delta\phi$ and $\bar{F}_1 \approx 1$. From Eq. (9.67), the growth rate for the dipole mode above transition can be written as

$$\frac{1}{\tau_1} = \mathcal{I}m\,\Omega = \frac{\eta e^2 NMR_s\omega_r}{2\beta^2 E_0\omega_s T_0^2} D(\alpha\tau_{\rm sep}) \ , \tag{9.72}$$

which agrees with the expression in Eq. (9.49) derived for short bunches. It is also evident from Fig. 9.7 that the excitations of higher azimuthal modes will be very much smaller.

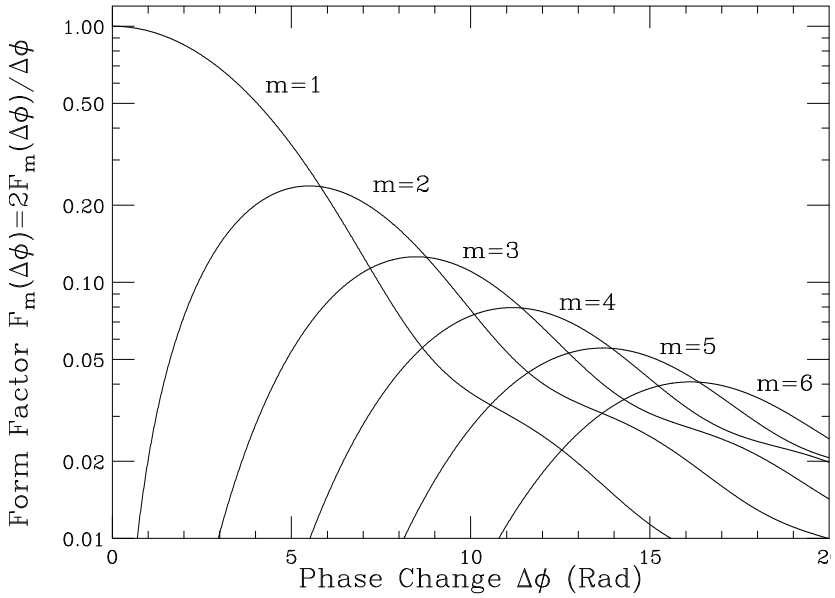

Figure 9.7: A more useful form factor $\bar{F}(\Delta\phi)$ in logarithmic scale for longitudinal oscillation inside a bunch with azimuthal modes $m = 1,\ 2,\ 3,\ 4,\ 5$ and 6. The unperturbed parabolic distribution in the longitudinal phase space is assumed. It is related to the Sacherer's form factor of Fig. 9.6 by $\bar{F}(\Delta\phi) = 2F(\Delta\phi)/\Delta\phi$.

9.3 Observation and Cures

The easiest way to observe longitudinal coupled-bunch instability is in a mountain-range plot, where bunches oscillate in a particular pattern as time advances. Examples are shown in Figs. 9.8 and 9.9. Streak camera can also be used to capture the phases of adjacent bunches as a function of time. From the pattern of coupling, the coupled-mode μ can be determined. From the frequency of oscillation, the azimuthal mode m can also be determined. We can then pin down the frequency $\omega_r/(2\pi)$ of the offending resonance driving the instability.

Observation can also be made in the frequency domain by zooming in the region between two rf harmonics in the way illustrated in Fig. 9.2. The coupled-bunch mode excited will be shown as a strong spectral line in between.

Longitudinal coupled-bunch instability will lead to an increase in bunch length and an increase in energy spread. For a light source, this translates into an increase in the spot size of the synchrotron light.

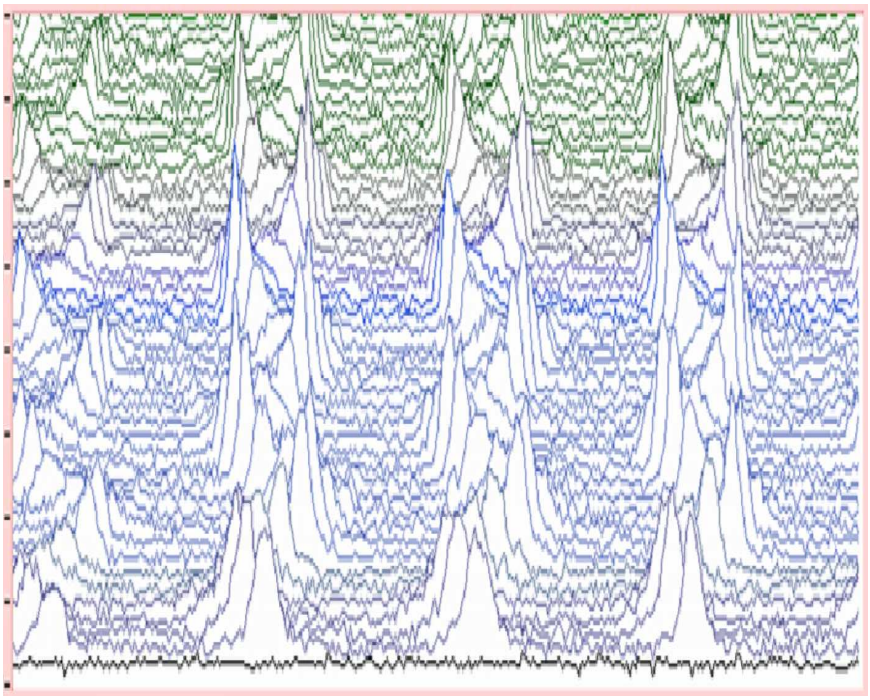

Figure 9.8: (color) Mountain-range plot showing coupled-bunch instability in the Fermilab Main Injector just after injection at 8 GeV.

There are many way to cure longitudinal coupled bunch instability. The driving resonances are often the higher-order modes inside the rf cavities. When the particular resonance is identified and if it is much narrower than the revolution frequency of the ring, we can try to shift its frequency so that it resides in between two revolution harmonics and becomes invisible to the beam particles. We can also study the electromagnetic field pattern of this resonance mode inside the cavity and install passive resistors and antennae to damp this particular mode. This method has been used widely in the Fermilab Booster, where longitudinal coupled-bunch instability had been very severe after the beam passed the transition energy. At that time, the bunch area increased almost linearly with bunch intensity. Passive damping of several offending modes cured this instability to such a point that the bunch area does not increase with bunch intensity anymore.

Longitudinal coupled-bunch instability had also been observed in the former Fermilab Main Ring. Besides passive damping of the cavity resonant modes, the instability was also reduced by lowering the rf voltage. Lowering the rf voltage will lengthen the bunch and reduce the form factor $F_m(\Delta\phi)$. This is only possible for a proton machine

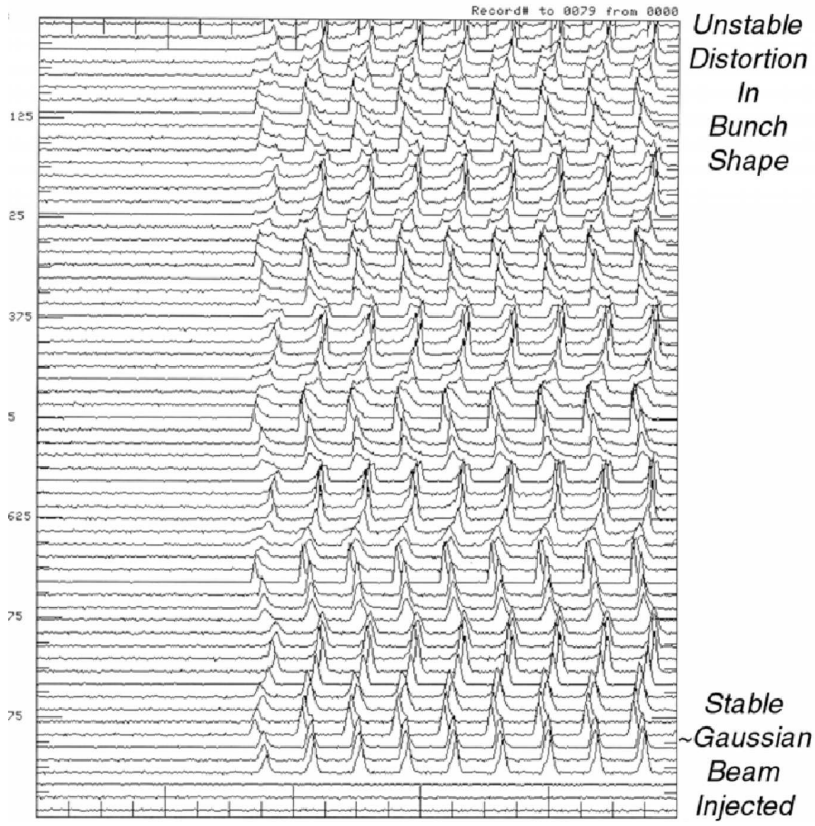

Figure 9.9: Mountain range plot showing bunches in a batch executing coupled-bunch instability in the Fermilab Main Injector just after injection at 8 GeV

where the bunches are long. It will not work for the short electron bunches for the $m = 1$ dipole mode. This is because, as mentioned before, the form factor for the dipole mode is not sensitive to the bunch length for short bunches. Even for a proton machine, the rf voltage cannot be reduced by a large amount because proton bunches are usually rather tight inside the rf bucket, especially during ramping.

If the growth turns out to be harmful, a fast bunch-by-bunch damper may be necessary to damp the dipole mode ($m = 1$). A damper for the quadrupole mode ($m = 2$) may also be necessary. This consists essentially of a wall-gap pickup monitoring the changes in bunch length and the corresponding excitation of a modulation of the rf waveform with roughly twice the synchrotron frequency. A feed-back correction is then made to the rf voltage. Another way to damp the longitudinal coupled-bunch instability is to break the symmetry between the M bunches. For example, a 5% to 10% variation in the intensity of the bunches will help. Another way to break the symmetry

is to have bunches not placed symmetrically in the ring. Some analysis shows that the stability will be improved if some bunches in the symmetric configuration are missing [3]. Prabhakar [4] recently proposed a new way to cure longitudinal coupled-bunch instability using uneven fill in a storage ring. We are going to discuss this method in more detail in Sec. 9.3.4.

There can also be Landau damping, which comes from the spread of the synchrotron frequency. The spread due to the nonlinear sinusoidal rf wave form as given by Eq. (9.51) is usually small unless the synchronous angle is large. Electron bunches are usually much smaller in size than the rf bucket. As a result, the spread in synchrotron frequency is be very minimal and does not help much in Landau damping.

9.3.1 Higher-Harmonic Cavity

In order to Landau damp longitudinal coupled-bunch instability, a large spread in synchrotron frequency inside the bunch is required. One way to do this is to install a higher-harmonic cavity, sometime known as *Landau cavity* [5] because it provides Landau damping. For example, the higher-harmonic cavity has resonant angular frequency $m\omega_{\rm rf}$ and voltage $rV_{\rm rf}$, where $\omega_{\rm rf}$ is the resonant angular frequency and $V_{\rm rf}$ the voltage of the fundamental rf cavity. The total rf voltage seen by the beam particles becomes

$$V(\tau) = V_{\rm rf}\big[\sin(\phi_s - \omega_{\rm rf}\tau) - r\sin(\phi_m - m\omega_{\rm rf}\tau)\big] - \frac{U_s}{e} \ , \tag{9.73}$$

where the phase angles ϕ_s and ϕ_m are chosen to compensate for U_s, the radiation energy loss, or to provide any required acceleration, We would like the bottom of the potential well, which is the integral of $V(\tau)$, to be as flat as possible. The rf voltage seen by the synchronous particle is compensated to zero by the energy lost to synchrotron radiation. In addition, we further require

$$\left.\frac{\partial V}{\partial \tau}\right|_{\tau=0} = 0 \qquad \text{and} \qquad \left.\frac{\partial^2 V}{\partial \tau^2}\right|_{\tau=0} = 0 \ , \tag{9.74}$$

so that the potential will become quartic instead. We therefore have 3 equations in 3 unknowns:

$$\sin\phi_s = r\sin\phi_m + \frac{U_s}{eV_{\rm rf}} \ , \tag{9.75}$$

$$\cos\phi_s = rm\cos\phi_m \ , \tag{9.76}$$

$$\sin\phi_s = rm^2\sin\phi_m \ , \tag{9.77}$$

from which ϕ_m and r can be solved easily (Exercise 9.5). For small-amplitude oscillation, the potential becomes

$$-\int V(\tau)d(\omega_{\rm rf}\tau) \longrightarrow \frac{m^2-1}{24}(\omega_{\rm rf}\tau)^4 V_{\rm rf}\cos\phi_s \ , \tag{9.78}$$

which is quartic and the synchrotron frequency is (Exercise 9.6)

$$\frac{\omega_s(\tau)}{\omega_{s0}} = \frac{\pi}{2}\left(\frac{m^2-1}{6}\right)^{1/2}\frac{\omega_{\rm rf}\tau}{K(1/\sqrt{2})}\left[\frac{1-\left(\dfrac{m^2}{m^2-1}\,\dfrac{U_s}{eV_{\rm rf}}\right)^2}{1-\left(\dfrac{U_s}{eV_{\rm rf}}\right)^2}\right]^{1/4} \ , \tag{9.79}$$

where the last factor can usually be neglected; its deviates from unity by only $\sim[(m^2-1)U_s/(2eV_{\rm rf})]^2$ if the synchronous angle is small. In above, ω_{s0} is the synchrotron angular frequency at zero amplitude when the higher-harmonic cavity voltage is turned off, and $K(1/\sqrt{2}) = 1.854$ is the complete elliptic integral of the first kind which is defined as

$$K(t) = \int_0^{\pi/2}\frac{d\theta}{\sqrt{1-t^2\sin^2\theta}} \ . \tag{9.80}$$

We see that the synchrotron frequency is zero at zero amplitude and increases linearly with amplitude. This large spread in synchrotron frequency may be able to supply ample Landau damping to the longitudinal coupled-bunch instability.

In the situation where there is no radiation loss and no acceleration, $U_s = 0$, the solution of Eqs. (9.75) to (9.77) simplifies, giving $\phi_s = \phi_m = 0$ and the ratio of the voltages of higher-harmonic cavity to the fundamental $r = 1/m$. Of course, it is also possible to have $r \neq 1/m$. Then the synchrotron frequency at the zero amplitude will not be zero and the spread in synchrotron frequency can still be appreciable. When $m = 2$, i.e., having a second-harmonic cavity, the mathematics simplifies. The synchrotron frequencies for various values of r are plotted in Fig. 9.10. Here, $r = 0$ implies having only the fundamental rf while $r = \frac{1}{2}$ the situation of having the synchrotron frequency linear in amplitude for small amplitudes. In between, the synchrotron frequency spread decreases as r decreases. Notice that for $0.3 \lesssim r < 0.5$, the synchrotron frequency has a maximum near the rf phase of $\sim 100°$. Particles near there will have no Landau damping at all and experience instability. Thus the size of the bunch is limited when a double cavity is used. Also the size of the bunch cannot be too small because of two reasons: first, the average synchrotron frequency may have been too low, and second, the central region of the phase space is a sea of chaos [7].

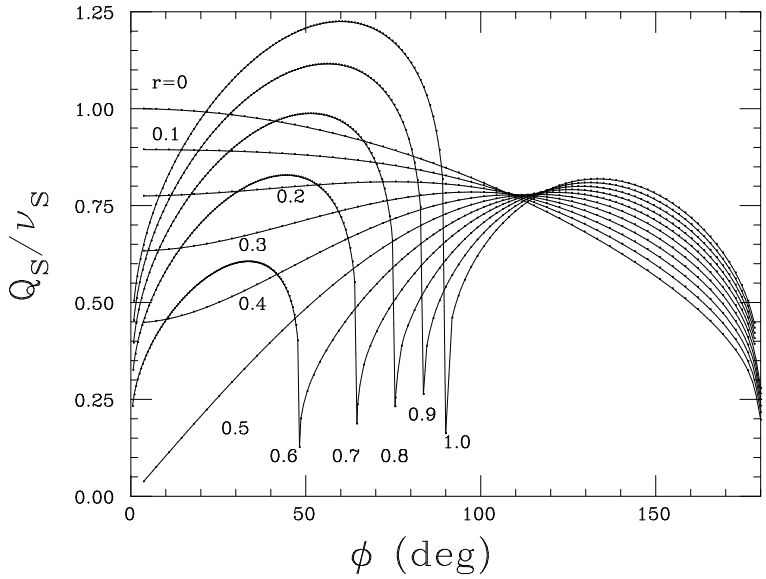

Figure 9.10: The normalized synchrotron tune of a double rf system as a function of the peak rf phase ϕ for various voltage ratio r. Here, the higher-harmonic cavity has frequency twice that of the fundamental. When $r > \frac{1}{2}$, the center of the bucket becomes an unstable fixed point and two stable fixed points emerge [7].

A Landau cavity increases the spread in synchrotron frequency, therefore it is ideal in damping mode-coupling instability and coupled-bunch instability. However, it may be not helpful for the Keil-Schnell type longitudinal microwave instability, which is valid for coasting beams. This method was first applied successfully with a third-harmonic cavity to increase Landau damping at the Cambridge Electron Accelerator (CEA) [8]. It was later applied to the Intersecting Storage Ring (ISR) at CERN SR a 6th harmonic cavity to cure mode-coupling instability [9]. Recently, a third-harmonic cavity has been reported in the SOLEIL ring in France to give a relative frequency spread of about 200%. However, since the center frequency has been dramatically decreased (not exactly to zero), the net result is a poor improvement in the stabilization. The gain in the stability threshold has been only 30% [6].

Actually, with a higher-harmonic cavity, the bunch becomes more rectangular-like in the longitudinal phase space, or particles are not so concentrated at the center of the bunch. Assuming the bunch area to be the same, the Boussard-modified Keil-Schnell threshold is proportional to the energy spread. Since the bunch becomes more flattened, the maximum energy spread which is at the center of the bunch is actually reduced, and

so will be the instability threshold. However, spreading out the particles longitudinally does help to increase the bunching factor and decrease the incoherent self-field or space-charge tune shift. At the CERN Proton Synchrotron Booster, an rf system with higher harmonics 5 to 10 has raised the beam intensity by about 25 to 30% [10]. For the Cooler Ring at the Indiana University Cyclotron Facility, a double cavity has been able to quadruple the beam intensity [7].

9.3.2 Passive Landau Cavity

Higher-harmonic cavities are useful in producing a large spread in synchrotron frequency so that single-bunch mode-mixing instability and coupled-bunch instability can be damped. However, the power source to drive this higher-harmonic rf system can be rather costly. One way to overcome this is to do away with the power source and let the higher-harmonic cavity or cavities be driven by the beam loading voltage of the circulating beam.

Let the ratio of the resonant frequencies of the higher-harmonic cavity to the fundamental rf cavity be m and the rf harmonic of the fundamental rf cavity be h. If the higher-harmonic cavity has a high quality factor, the beam loading voltage is just i_b, the current component at the cavity resonant frequency, multiplied by the impedance of the cavity. Here, for a Gaussian bunch

$$i_b = 2I_0 e^{-\frac{1}{2}(mh\omega_0\sigma_\tau)^2} \ , \tag{9.81}$$

where σ_τ is the rms bunch length and ω_0 is the angular revolution frequency. Thus for a short bunch, $i_b \approx 2I_0$ with I_0 being the average current of the bunch.

The higher-harmonic cavity must have suitable shunt impedance R_s and quality factor Q, and this can be accomplished by installing necessary resistor across the cavity gap. Thus, R_s and Q can be referred to as the loaded quantities of the cavity. For a particle arriving at time τ ahead of the synchronous particle, it sees the total voltage

$$V(\tau) = V_{\rm rf}\sin(\phi_s - \omega_{\rm rf}\tau) - i_b R_s \, \mathcal{R}e\left[\frac{1}{1+i2Q\delta}e^{im\omega_{\rm rf}\tau}\right] - \frac{U_s}{e} \ , \tag{9.82}$$

where $\omega_{\rm rf} = h\omega_0$ is the angular rf frequency determined by the resonator in the rf klystron that drives the fundamental rf cavity and the negative sign in front of i_b indicates that

this beam loading voltage is induced by the image current and opposes the beam current. In above,

$$\delta = \frac{1}{2}\left(\frac{\omega_r}{m\omega_{\rm rf}} - \frac{m\omega_{\rm rf}}{\omega_r}\right) \approx \frac{\omega_r - m\omega_{\rm rf}}{\omega_r} \tag{9.83}$$

represents the deviation of the resonant angular frequency ω_r of the higher-harmonic cavity from the mth multiple of the rf angular frequency. Of course, this is related to the detuning angle ψ of the higher-harmonic cavity, which we introduce in the usual way as

$$\tan\psi = 2Q\delta \ . \tag{9.84}$$

Now, Eq. (9.82) can be rewritten as

$$V(\tau) = V_{\rm rf}\sin(\phi_s - \omega_{\rm rf}\tau) - i_b R_s \cos\psi\cos(\psi - m\omega_{\rm rf}\tau) - \frac{U_s}{e} \ . \tag{9.85}$$

Again to acquire the largest spread in synchrotron frequency, we require

$$V(0) = 0\,, \quad V'(0) = 0\,, \quad V''(0) = 0\,, \tag{9.86}$$

so that the potential for small amplitudes becomes quartic,

$$U(\tau) = -\int V(\tau)d\tau = -\frac{\tau^4}{4!}V'''(0) \ . \tag{9.87}$$

Since we are having exactly the same quartic potential as in an rf system with an active Landau cavity, we expect the synchrotron frequency to be exactly the same as the expression given by Eq. (9.79) when the oscillation amplitude is small.

The set of requirements, however, are different from that of the active Landau cavity system. Here, the requirements are

$$V_{\rm rf}\sin\phi_s \ = \ i_b R_s\cos^2\psi + U_s/e \ , \tag{9.88}$$

$$V_{\rm rf}\cos\phi_s \ = \ -m\, i_b R_s\cos\psi\sin\psi \ , \tag{9.89}$$

$$V_{\rm rf}\sin\phi_s \ = \ m^2 i_b R_s\cos^2\psi \ . \tag{9.90}$$

For an electron machine which is mostly above transition, the synchronous angle ϕ_s is between $\frac{1}{2}\pi$ and π. Thus, from Eq. (9.89), we immediately obtain

$$\sin 2\psi > 0 \Longrightarrow 0 < \psi < \frac{\pi}{2} \ , \tag{9.91}$$

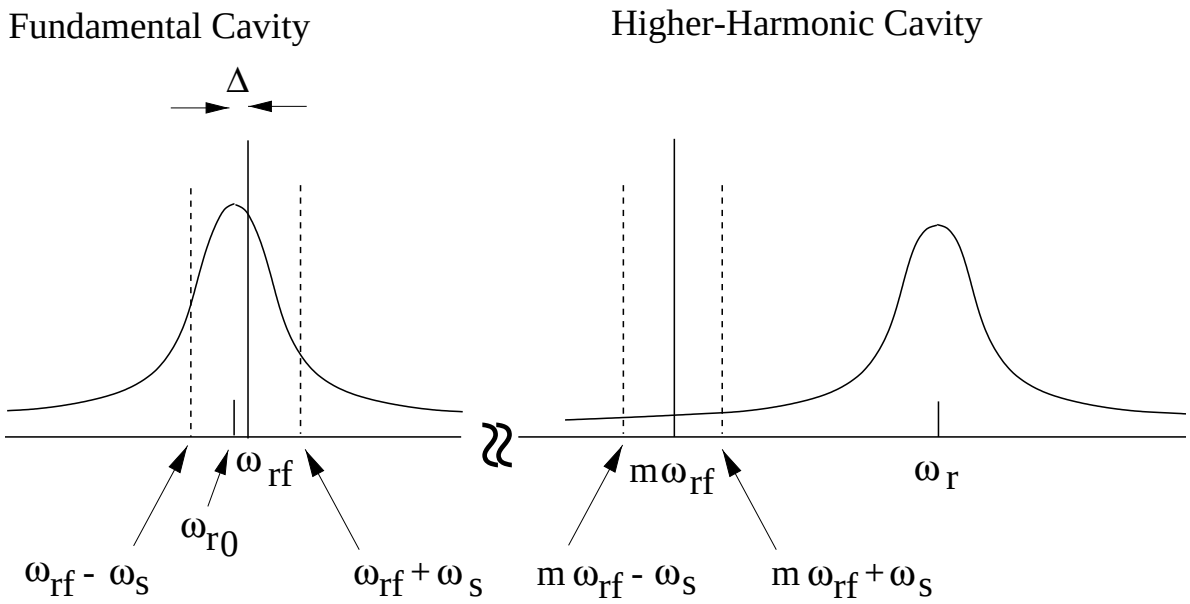

Figure 9.11: For the higher-harmonic cavity, the resonant frequency ω_r is above the mth multiple of the rf frequency. The beam will be Robinson unstable above transition. For the fundamental cavity, the resonant frequency ω_{r0} is below the rf frequency $\omega_{\rm rf} = h\omega_0$, and the beam will be Robinson stable. The detuning of the fundamental rf should be so chosen that the beam will be stable after traversing both cavities.

and from Eqs. (9.83) and (9.84), $\omega_r > m\omega_{\rm rf}$. This means that the beam in the higher-harmonic cavity is Robinson unstable [4], as is illustrated in Fig. 9.11. Of course, the fundamental rf cavity should be Robinson stable, and it will be nice if the detuning is so chosen that the beam remains stable after traversing both cavities.

The synchrotron light source electron ring at LNLS, Brazil would like to install a passive Landau cavity with $m = 3$ in order to alleviate the longitudinal coupled-bunch instabilities. The fundamental rf system has harmonic $h = 148$ or rf frequency $f_{\rm rf} = \omega_{\rm rf}/(2\pi) = 476.0$ MHz with a tuning range of ± 10 kHz, and rf voltage $V_{\rm rf} = 350$ kV. To overcome the radiation loss, the synchronous phase is set at $\phi_{s0} = 180^\circ - 19.0^\circ$. This gives a synchrotron tune at small amplitudes $\nu_s = 6.87 \times 10^{-3}$ or a synchronous frequency $f_s = 22.1$ kHz.

With the installation of the passive Landau cavity, the synchronous phase must be modified to a new ϕ_s, which is obtained by solving Eqs. (9.88) and (9.90):

$$\sin\phi_s = \left(\frac{m^2}{m^2-1}\right)\left(\frac{U_s}{eV_{\rm rf}}\right) = \frac{m^2}{m^2-1}\sin\phi_{s0} \ . \tag{9.92}$$

Thus,

$$\phi_{s0} = 180^\circ - 19.0^\circ \quad \Longrightarrow \quad \phi_s = 180^\circ - 21.49^\circ \ , \tag{9.93}$$

where $m = 3$ has been used. The detuning ψ of the higher-harmonic cavity can be obtained from Eqs. (9.89) and (9.90), or

$$\tan\psi = -m\cot\phi_s \quad \Longrightarrow \quad \psi = 82.53^\circ \ . \tag{9.94}$$

Finally from Eq. (9.90),

$$i_b R_s = \frac{V_{\rm rf}\sin\phi_s}{m^2\cos^2\psi} \ . \tag{9.95}$$

With $i_b = 2I_0 = 0.300$ A and $V_{\rm rf} = 350$ kV, we obtain the shunt impedance of the higher-harmonic cavity to be $R_s = 2.81$ MΩ. The power taken out from the beam is

$$P = \frac{1}{2}\,\frac{i_b^2 R_s}{1+\tan^2\psi} = 2.14 \text{ kW} \ , \tag{9.96}$$

which is not large when compared with the power loss due to radiation

$$P_{\rm rad} = NU_s f_0 = I_0 V_{\rm rf}\sin\phi_{s0} = 17.09 \text{ kW} \ , \tag{9.97}$$

where N is the number of electrons in the bunch. The higher-harmonic cavity has a quality factor of $Q = 45000$ and a resonant frequency $f_r \sim 3f_{r0} = 1428$ MHz. From the detuning, it can easily found that the frequency offset is $f_r - 3f_{\rm rf} = 121$ kHz.

Now let us compute the growth rate for one bunch at the coherent frequency Ω. For one particle of time advance τ, we have from Sacherer's integral equation for a short bunch [2],

$$\Omega^2 - \omega_s(\tau)^2 = \frac{i\eta e I_0}{E_0 T_0}\sum_q (q\omega_0+\Omega) Z_0^{\parallel}(q\omega_0+\Omega) \ . \tag{9.98}$$

where η is the slip factor and we have retained the dependency of the synchrotron frequency ω_s on τ because of its large spread in the presence of the higher-harmonic cavity. From Eq. (9.79), this dependency is

$$\frac{\omega_s(\tau)}{\omega_{s0}} = \frac{\pi}{2}\left(\frac{m^2-1}{6}\right)^{1/2}\frac{\omega_{\rm rf}\tau}{K(1/\sqrt{2})}\sqrt{\frac{\cos\phi_s}{\cos\phi_{s0}}} \ , \tag{9.99}$$

where the last factor amounts to 0.9920 and can therefore be safely abandoned. Thus, the average ω_s^2 over the whole bunch just gives the square of the rms frequency spread,

$$\langle\omega_s^2\rangle = \sigma_{\omega_s}^2 = \left[\frac{\pi\omega_{s0}}{2}\sqrt{\frac{m^2-1}{6}}\frac{\omega_{\rm rf}\sigma_\tau}{K(1/\sqrt{2})}\right]^2 \ . \tag{9.100}$$

The FWHM natural bunch length at $V_{\rm rf} = 350$ kV is $\tau_{\rm FWHM} = 70.6$ ps; thus $\sigma_\tau = 30.0$ ps. This gives $\sigma_{\omega_s} = \tau_{\rm FWHM}/(2\sqrt{2\ln 2}) = 12.2$ kHz.

Since the synchrotron frequency is now a function of the offset from the stable fixed point of the rf bucket, a dispersion relation can be obtained from Eq. (9.98) by integrating over the synchrotron frequency distribution of the bunch. Here, we are interested in the growth rate without Landau damping, which is given approximately by

$$\begin{aligned}\frac{1}{\tau} = \mathcal{I}m\,\Omega \approx \frac{\eta e I_0\omega_{\rm rf}}{2E_0T_0(2\sigma_{\omega_s})}\Big\{&\Big[\mathcal{R}e\,Z_0^{\parallel}(\omega_{\rm rf}+2\sigma_{\omega_s}) - \mathcal{R}e\,Z_0^{\parallel}(\omega_{\rm rf}-2\sigma_{\omega_s})\Big] \\ &+ m\Big[\mathcal{R}e\,Z_0^{\parallel}(m\omega_{\rm rf}+2\sigma_{\omega_s}) - \mathcal{R}e\,Z_0^{\parallel}(m\omega_{\rm rf}-2\sigma_{\omega_s})\Big]\Big\} \ ,\end{aligned} \tag{9.101}$$

where the mean angular synchrotron frequency has been assumed to be

$$\bar{\omega}_s = 2\sigma_{\omega_s} \ . \tag{9.102}$$

The growth rate can be computed easily by substituting into Eq. (9.101) the expression for $\mathcal{R}e\,Z_0^{\parallel}$. However, the differences in Eq. (9.101) can also be approximated by derivatives. For the higher-harmonic cavity, both the upper and lower synchrotron sidebands lie on the same side of the higher-harmonic resonance as indicated in Fig. 9.11. Their difference, $\sim 4\sigma_{\omega_s}/(2\pi) = 7.76$ kHz, is also very much less than the cavity detuning $(\omega_r - m\omega_{\rm rf})/(2\pi) = 121$ kHz. Recalling that

$$\mathcal{R}e\,Z_0^{\parallel}(\omega) = R_s\cos^2\psi \ , \tag{9.103}$$

where the detuning ψ is given by Eq. (9.84), the second term can be written as a differential,

$$\mathcal{R}e\,Z_0^{\parallel}(m\omega_{\rm rf}+2\sigma_{\omega_s}) - \mathcal{R}e\,Z_0^{\parallel}(m\omega_{\rm rf}-2\sigma_{\omega_s}) \approx \left[R_s\cos^2\psi\sin 2\psi\,\frac{2Q}{\omega_r}\right]4\sigma_{\omega_s} \ . \tag{9.104}$$

For the fundamental cavity, the resonant frequency is $\omega_{r0}/(2\pi) = 476.00$ MHz. The detuning is usually $\Delta = -10$ kHz at injection and is reduced to $\Delta = -2$ kHz in

storage mode when the highest electron energy is reached. Thus, the upper and lower synchrotron sidebands lie on either side of the resonance as illustrated in Fig. 9.11. Since $\Delta \ll \sigma_{\omega_s}$, we can also write the first term of Eq. (9.101) as a differential about $\omega_{r0} + \bar{\omega}_s$, with the assumption that the resonance is symmetric about the resonant frequency ω_{r0}. Thus,

$$\mathcal{R}e\, Z_0^{\parallel}(\omega_{\rm rf} + \bar{\omega}_s) - \mathcal{R}e\, Z_0^{\parallel}(\omega_{\rm rf} - \bar{\omega}_s)$$

$$= \mathcal{R}e\, Z_0^{\parallel}(\omega_{r0} + \Delta + \bar{\omega}_s) - \mathcal{R}e\, Z_0^{\parallel}(\omega_{r0} - \Delta + \bar{\omega}_s) \approx \left[R_s \cos^2\psi_{\omega_s} \sin 2\psi_{\omega_s} \frac{2Q}{\omega_{r0}} \right] 2\Delta \ , \quad (9.105)$$

where ψ_{ω_s}, which is similar to a detuning angle by the amount $\bar{\omega}_s$, is defined as

$$\tan\psi_{\omega_s} = 2Q \frac{\bar{\omega}_s}{\omega_{r0}} \ . \quad (9.106)$$

We arrive at

$$\frac{1}{\tau} = \frac{2\eta e I_0 Q}{E_0 T_0} \left[\frac{\Delta}{\bar{\omega}_s} \ R_s \cos^2\psi_{\omega_s} \sin 2\psi_{\omega_s}\big|_{\rm fund} + R_s \cos^2\psi \sin 2\psi\big|_{\rm higher} \right] \ , \quad (9.107)$$

where the contributions from the fundamental and higher-harmonic cavities are indicated by the subscripts 'fund' and 'higher', respectively. The square bracketed factor in Eq. (9.107) becomes

$$\left[\frac{\Delta}{\bar{\omega}_s} \ R_s \cos^2\psi_{\omega_s} \sin 2\psi_{\omega_s}\big|_{\rm fund} + R_s \cos^2\psi \sin 2\psi\big|_{\rm higher} \right] = (-0.1953 + 0.0122)\ {\rm M}\Omega \ , \quad (9.108)$$

where we have used for the fundamental cavity, the shunt impedance $R_s = 3.84\ {\rm M}\Omega$, and quality factor $Q = 45000$ exactly the same as the higher harmonic cavity. The two-rf system turns out to be Robinson stable; the damping rate is $54600\ {\rm s}^{-1}$ or a damping time of 0.018 ms. However, it is important to point out that the growth rate formula given by Eq. (9.101) is valid only if the shift and spread of the synchrotron frequency are much less than some unperturbed synchrotron frequency. Here, the synchrotron frequency is linear with the offset from the stable fixed point of the longitudinal phase space and the spread is therefore very large. Thus, Eq. (9.101) can only be viewed as an estimate. The employment of a mean synchrotron angular frequency $\bar{\omega}_s$ can also be questionable. Although the assumption of the mean synchrotron angular frequency in Eq. (9.102) is not sensitive to the higher-harmonic-cavity term in Eq. (9.101), however, it is rather sensitive to the fundamental-cavity term. The dependence is complicated since the equivalent detuning ψ_{ω_s} depends on $\bar{\omega}_s$ also. For example, if we use $\bar{\omega}_s = 1.5\sigma_{\omega_s}$ instead,

the damping time decreases to 0.013 ms, while $\bar{\omega}_s = 3.0\sigma_{\omega_s}$ increases the damping time to 0.036 ms. With this uncertainty, a suggestion may be to increase the detuning Δ of the fundamental to $\Delta \sim -4$ kHz so that it becomes more certain that the two-rf system will be Robinson stable, otherwise, the purpose of the higher-harmonic cavity can be defeated, because some of the spread of the synchrotron frequency obtained will be used to fight the Robinson's instability created instead of other longitudinal collective instabilities of concern.

Now let us estimate how large a Landau damping we obtain from the passive Landau cavity coming from the spread of the synchrotron frequency. Following Eq. (9.52), the stability criterion is roughly

$$\frac{1}{\tau} \lesssim \frac{\omega_s(\sqrt{6}\sigma_\tau)}{4} \ , \tag{9.109}$$

where the synchrotron angular frequency spread is given by Eq. (9.79). The spread in synchrotron angular frequency has been found to be $\omega_s(\sqrt{6}\sigma_\tau) = 39.6$ kHz. In other words, the higher-harmonic cavity is able to damp an instability that has a growth time longer than 0.101 ms, an improvement of 57 folds better than when the higher-harmonic cavity is absent. Thus, theoretically, this Landau damping is large enough to alleviate the Robinson's antidamping of higher-harmonic cavity as well.

We notice that the required shunt impedance of the passive Landau cavity $R_s = 2.81$ MΩ is large, although it is still smaller than the shunt impedance of 3.84 MΩ of the fundamental cavity. It is easy to understand why such large impedance is required. The synchronous angle for a storage ring without the Landau cavity is usually just not too much from 180°, here $\phi_{s0} = 180° - 19.0°$, because of the compensation of a small amount of radiation loss. The rf gap voltage phasor is therefore almost perpendicular to the beam current phasor. In order that the beam loading voltage contributes significantly to the rf voltage, the detuning angle of the passive higher-harmonic cavity must therefore be large also, here $\psi = 82.53°$. In fact, without radiation loss to compensate, the beam loading voltage phasor would have been exactly perpendicular to the beam current phasor. Since $\cos\psi = 0.130$ is small, the shunt impedance of the higher-harmonic cavity must therefore be large. In some sense, the employment of the higher-harmonic cavity is not efficient at all, because we are using only the tail of a large resonance impedance, as is depicted in Fig. 9.11. This is not a waste at all, however, because we can do away with the generator power source for this cavity. Also, the large detuning angle implies not much power will be taken out from the beam as it loads the cavity, only 2.14 kW here. On the other hand, the detuning of the fundamental cavity need not be too large. This is because

the rf gap voltage is supplied mostly by the generator voltage and only partially by the beam loading in the cavity.

The most important question here is how do we generate a large shunt impedance for the higher-harmonic cavity. Usually it is easy to lower the shunt impedance by adding a resistor across the cavity gap. Some other means will be required to raise the shunt impedance, in case it is not large enough. One way is to coat the interior of the higher-harmonic cavity with a layer of medium that has a higher conductivity. However, it is hard to think of any medium that has a conductivity very much higher than that of the copper surface of the cavity. For example, the conductivity of silver is only slightly higher. Another way to increase the conductivity significantly is the reduction of temperature to the cryogenic region. Notice that R_s/Q is a geometric property of the cavity. Raising R_s will raise Q also. However, a higher quality factor is of no concern here, because the requirements in Eqs. (9.88), (9.89), and (9.90) depend on the detuning ψ only and are independent of Q. With the same detuning ψ, a higher Q just implies a smaller frequency offset between the resonant angular frequency ω_r of the higher-harmonic cavity and the mth multiple of the rf angular frequency.

The shunt impedance of the higher-harmonic cavity determines the rf voltage to be used in the fundamental cavity. We can rewrite Eq. (9.95) as

$$\frac{i_b R_s}{U_s/e} = \left(\frac{m^2-1}{m^2}\right)\left(\frac{V_{\rm rf}}{U_s/e}\right)^2 - 1 \ , \tag{9.110}$$

after eliminating ϕ_s and ψ with the aid of Eqs. (9.92) and (9.94). Thus, for a given beam current, a small shunt impedance of the higher-harmonic cavity translates into small rf voltage. Notice that the right side is quadratic in $V_{\rm rf}$. For example, with the same radiation loss, when the shunt impedance of the higher-order cavity decreases from 6.12 to 2.81 MΩ, the rf voltage $V_{\rm rf}$ has to decrease from 500 kV to 350 kV. A low rf voltage is usually not favored because the electron bunches will become too long.

In order to maximize Landau damping, criteria must be met so that the rf potential becomes quartic. As is shown in Fig. 9.10 for a $m = 2$ double rf system, when the rf voltage ratio deviates from $r = 1/m = 0.5$ by 20% to 0.4, the spread in synchrotron frequency for a small bunch decreases tremendously to almost the same tiny value as in the single rf system. There is a big difference between an active Landau cavity and a passive Landau cavity. In an active Landau cavity, the criteria in Eqs. (9.77) to (9.77) are independent of the beam intensity. On the other hand, the criteria for the operation of a passive cavity, Eqs. (9.88), (9.89), and (9.90), depend on the bunch intensity. What

will happen when the bunch intensity changes significantly? Let us recall how we arrive at the solution of the three equations of the passive two-rf system. The new synchronous phase ϕ_s, as given by Eq. (9.92), is determined solely by the ratio of the radiation loss U_s to the rf voltage $V_{\rm rf}$. while the detuning ψ is just given by $-m\cot\phi_s$. The only parameter that depends on the beam current is the shunt impedance R_s. Thus, the easiest solution is to install a variable resistor across the the gap of the higher-harmonic cavity and adjust the proper shunt impedance by monitoring the intensity of the electron bunches.

In the event that the shunt impedance is not adjustable, one can adjust instead the rf voltage so that Eq. (9.110) remains satisfied with the new current but with the preset R_s. With the new rf voltage, the synchronous phase ϕ_s has to be adjusted so that Eq. (9.92) remains satisfied. This will alter the detuning ψ according to Eq. (9.94). The only way to achieve the new detuning is to vary the rf frequency. This will push the beam radially inward or outward. As the beam current changes by $\Delta I_0/I_0$, to maintain the criteria of the quartic rf potential, the required changes in rf voltage, synchronous angle, and detuning of the higher-harmonic cavity are, respectively,

$$\frac{\Delta V_{\rm rf}}{V_s} = \frac{1}{2}\left[\frac{m^2}{m^2-1}\frac{V_s}{V_{\rm rf}}\right]\left[\frac{m^2-1}{m^2}\frac{V_{\rm rf}^2}{V_s^2}-1\right]\frac{\Delta I_0}{I_0}\ , \tag{9.111}$$

$$\Delta(\pi-\phi_s) = -\left[\left(\frac{m^2-1}{m^2}\frac{V_{\rm rf}}{V_s}\right)^2-1\right]^{-1/2}\frac{\Delta V_{\rm rf}}{V_s}\ , \tag{9.112}$$

$$\Delta\psi = \frac{1}{2m}\left[\left(\frac{m^2-1}{m^2}\frac{V_{\rm rf}}{V_s}\right)^2-1\right]^{-1/2}\frac{\Delta I_0}{I_0}\ , \tag{9.113}$$

where $U_s = eV_s$ is the energy loss per turn due to synchrotron radiation. The change of the detuning angle ψ leads to a fractional change in the rf frequency and therefore a fractional change in orbit radius

$$\frac{\Delta R}{R} = -\frac{m^2-1}{4mQ}\left[\frac{m^2-1}{m^2}\frac{V_{\rm rf}^2}{V_s^2}-1\right]\left[\left(\frac{m^2-1}{m^2}\frac{V_{\rm rf}}{V_s}\right)^2-1\right]^{-1/2}\frac{\Delta I_0}{I_0}\ , \tag{9.114}$$

where R is the radius of the storage ring. These changes are plotted in Fig. 9.12 for the LNLS double rf system when he beam current varies by $\pm 20\%$. Because of the high quality factors Q of the cavities, the radial offset of the beam turns out to be very small, less than ± 0.14 mm for a $\pm 20\%$ variation of beam current.

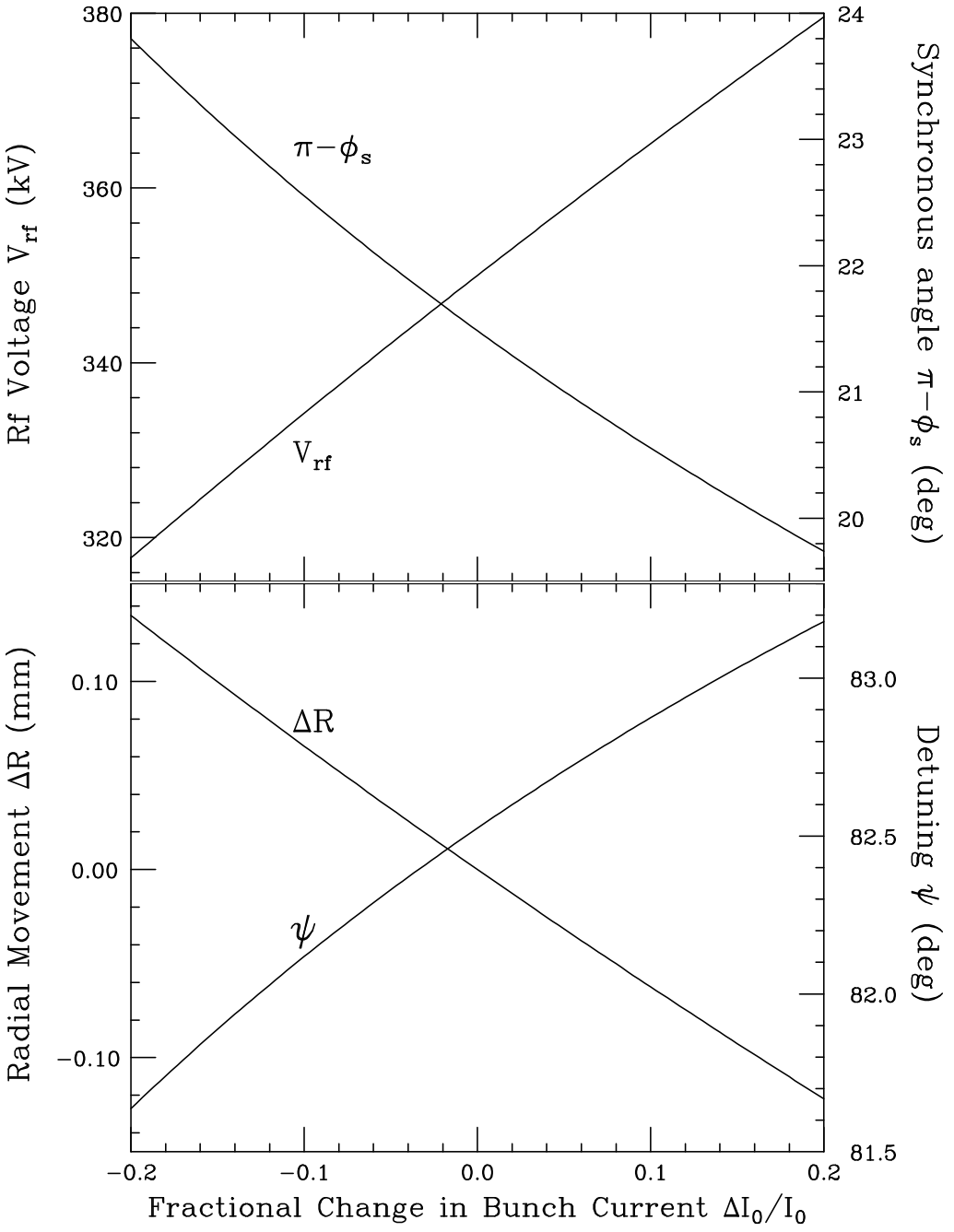

Figure 9.12: Plots showing the required variations of rf voltage $V_{\rm rf}$, synchronous angle ϕ_s, higher-harmonic-cavity detuning ψ, and beam radial offset Δr to maintain the criteria of the quartic rf potential, when the beam current varies by $\pm 20\%$.

9.3.3 Rf Voltage Modulation

The modulation of the rf system will create nonlinear parametric resonances, which redistribute particles in the longitudinal phase plane. The formation of islands within an rf bucket reduces the density in the bunch core and decouples the coupling between bunches. As a result, beam dynamics properties related to the bunch density, such as beam lifetime, beam collective instabilities, etc, can be improved.

Here we try to modulate the rf voltage with a frequency $\nu_m\omega_0/(2\pi)$ and amplitude ϵ, so that the energy equation becomes [11]

$$\frac{d\Delta E}{dn} = eV_{\rm rf}[1+\epsilon\sin(2\pi\nu_m n+\xi)][\sin(\phi_s-h\omega_0\tau)-\sin\phi_s]-[U(\delta)-U_s]\ , \qquad (9.115)$$

where ξ is a randomly chosen phase, ν_m is the modulating tune, ϵ is the fractional voltage modulation amplitude, U_s and $U(\delta)$ denote the energy loss due to synchrotron radiation for the synchronous particle and a particle with momentum offset δ. This modulation will introduce resonant-island structure in the longitudinal phase plane. There are two critical tunes:

$$\begin{cases} \nu_1 = 2\nu_s + \frac{1}{2}\epsilon\nu_s\ , \\ \nu_2 = 2\nu_s - \frac{1}{2}\epsilon\nu_s\ . \end{cases} \qquad (9.116)$$

If we start the modulation by gradually increasing the modulating tune ν_m towards ν_2 from below, two islands appear inside the bucket from both sides, as shown in the second plot of Fig. 9.13. The phase space showing the islands is depicted in Fig. 9.14. As ν_m is increased, these two islands come closer and closer to the center of the bucket and the particles in the bunch core gradually spill into these two islands, forming 3 beamlets. When ν_m reaches ν_2, the central core disappears and all the particles are shared by the two beamlets in the two islands. Further increase of ν_m above ν_2 moves the two beamlets closer together. When ν_m equals ν_1, the two beamlets merge into one. Under all these situations, the two outer islands rotate around the center of the rf bucket with frequency equal to one half the modulation frequency. Every rf bucket has the same phase space structure of having two or three islands rotating at the same angular velocity and with the roughly same phase. The only possible small phase lag is due to time-of-flight. Therefore, only coupled mode $\mu = 0$ will be allowed, unless the driving force is large enough to overcome the voltage modulation.

Rf voltage modulation has been introduced into the light source at the Synchrotron Radiation Research Center (SRRC) of Taiwan to cope with longitudinal coupled-bunch

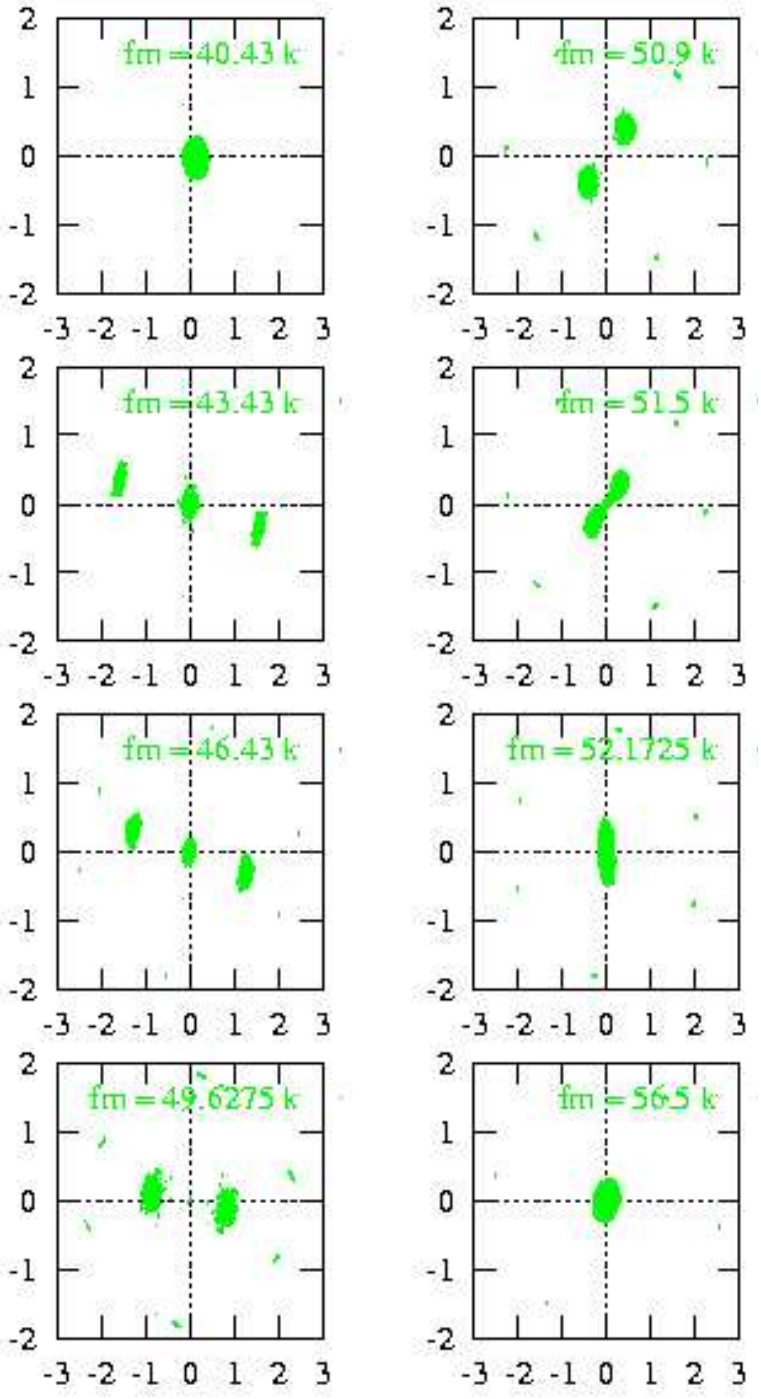

Figure 9.13: (Color) Simulation results of rf voltage modulation. The modulation frequency is increased from top to bottom and left to right. The modulation amplitude is 10% of the cavity voltage. The 4th plot is right at critical frequency $\nu_2 f_0 = 49.6275$ kHz and the 7th plot right at critical frequency $\nu_1 f_0 = 52.1725$ kHz.

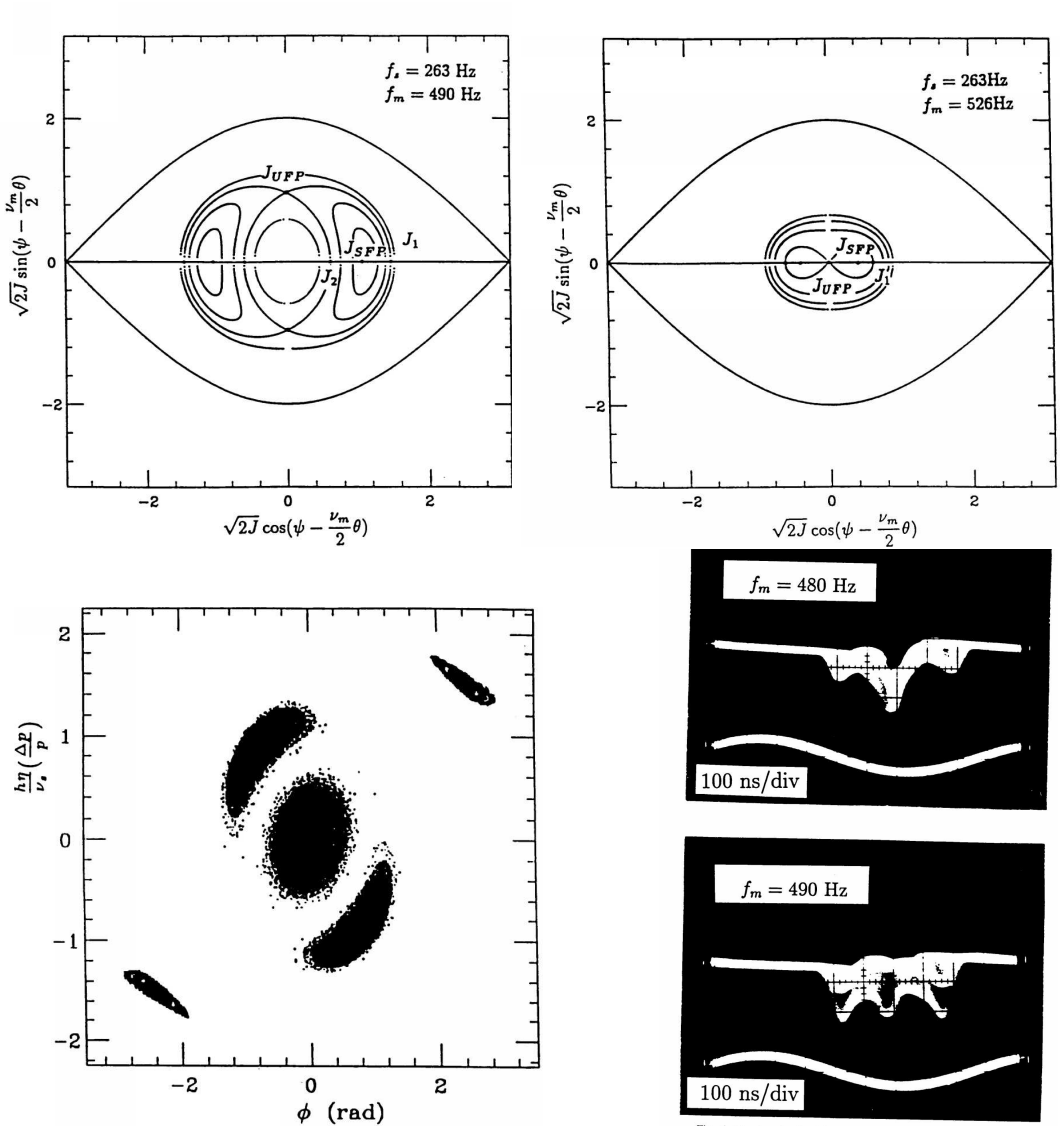

Figure 9.14: Top figures show separatrices and tori of the time-independent Hamiltonian with voltage modulation in multi-particle simulation for an experiment at Indiana University Cyclotron Facility. The modulation tune is below ν_2 with the formation of 3 islands on the left, while the modulation tune is above ν_2 with the formation of 2 islands on the right. The lower-left plot shows the final beam distribution when there are 3 islands, a damping rate of 2.5 s^{-1} has been assumed. The lower-right plot shows the longitudinal beam distribution from a BPM sum signal accumulated over many synchrotron periods. Note that the outer two beamlets rotate around the center beamlet at frequency equal to one-half the modulation frequency.

instability [12]. The synchrotron frequency was $\nu_s f_0 = 25.450$ kHz. A modulation frequency slightly below twice the synchrotron frequency with $\epsilon = 10\%$ voltage modulation was applied to the rf system. The beam spectrum measured from the beam-position monitor (BPM) sum from a HP4396A network analyzer before and after the modulation is shown in Fig. 9.15. It is evident that the intensities of the beam spectrum at the annoying frequencies have been largely reduced after the application of the modulation. The sidebands around the harmonics of 587.106 Hz and 911.888 MHz are magnified in Fig. 9.16. We see that the synchrotron sidebands have been suppressed by very much. The multi-bunch beam motion under rf voltage modulation was also recorded by streak camera, which did not reveal any coupled motion of the bunches. Because of the successful damping of the longitudinal coupled-bunch instabilities, this modulation process has been incorporated into the routine operation of the light source at SRRC.

9.3.4 Uneven Fill

In a storage ring with M identical bunches evenly spaced, there will be M modes of coupled-bunch oscillation, of which about half are stable and half unstable in the presence of an impedance, if all other means of damping are neglected. Take the example of having the rf harmonic $h = M = 6$ as illustrated in Fig. 9.2. If there is a narrow resonant impedance in the rf cavity located at $\omega_r \approx (qM + \mu)\omega_0$ with $\mu = 4$, coupled-bunch mode $\mu = 4$ becomes highly unstable. At the same time, this resonant impedance also damps coupled-bunch mode $M - \mu = 2$ heavily. Usually, we only care for the mode that is unstable and pay no attention the mode that is damped. In some sense, the damping provided by the impedance is rendered useless or has been wasted. However, if there is another narrow resonant impedance located at the angular frequency $(qM + \mu')\omega_0$ with $\mu' = 2$. This impedance excites coupled-bunch mode 2, but damps coupled-bunch mode 4. If this impedance is of the same magnitude as the first one, both coupled-bunch modes 2 and 4 can become stable. Thus, having more narrow resonances in the impedance does not necessarily imply more instabilities. If they are located at the desired frequencies, they can be helping each other so that the excitation of one can be canceled by the other. This method of curing coupled-bunch instability was proposed in Ref. [13] by creating extra resonances in the impedance in the accelerator ring. However, extra resonances in the impedance are not necessary. The same purpose can also be served if we can couple the two coupled-bunch modes together, for example modes 2 and 4 in the above example, the damped mode will be helping the growth mode. If the resulting growth

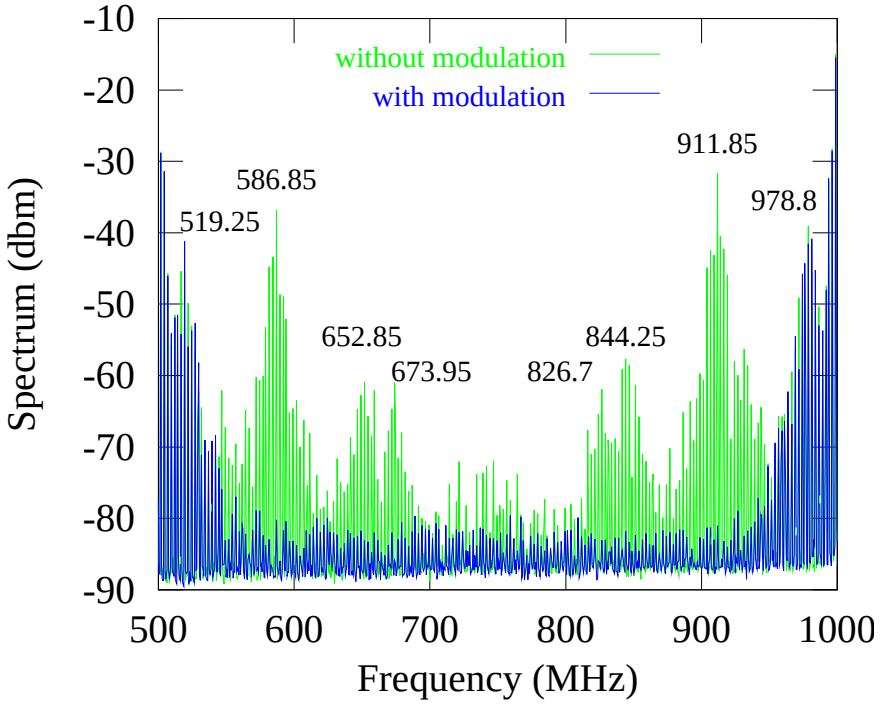

Figure 9.15: (Color) Beam spectrum from BPM sum signal before and after applying rf voltage modulation. The synchrotron frequency was 25.450 kHz. The voltage was modulated by 10% at 50.155 kHz. The frequency span of the spectrum is 500 MHz, which is the rf frequency.

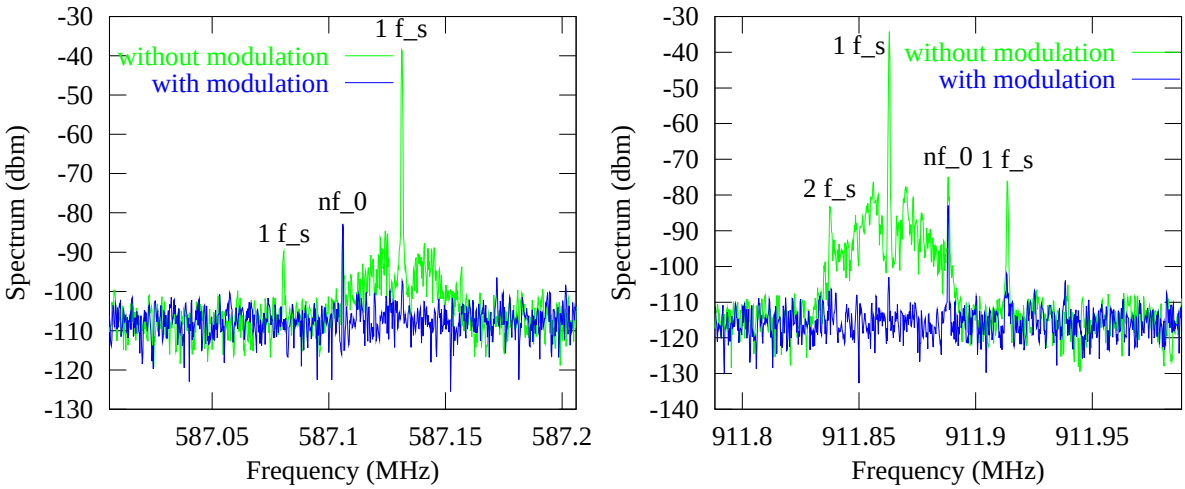

Figure 9.16: (Color) Beam spectrum zoom in from Fig. 9.15. The revolution harmonic frequency of the left is 587.106 MHz and the right is 911.888 MHz. The frequency span of the spectrum is 200 kHz.

rates of the two coupled modes fall lower than the synchrotron radiation damping rate and the Landau damping rate in the ring, the coupled-bunch instability will be cured. This method of cure is called *modulating coupling* proposed by Prabhakar [4, 14], and the coupling is accomplished with an uneven fill in the ring. We saw in Eq. (9.48) that wake field left by previous bunch passages contributes to a coherent synchrotron tune shift in the bunch. For an unevenly filled ring, the tune shifts for different bunches will be different. This provides a spread in synchrotron tune and therefore extra Landau damping, which is another idea proposed by Prabhakar.

Let us go over the uneven-fill theory briefly. Consider M point bunches evenly placed in the ring, but they may carry different charges. The arrival time advance τ_n of the nth bunch at time s obeys the equation of motion,

$$\ddot{\tau}_n + 2d_r\dot{\tau}_n + \omega_s^2\tau_n = \frac{e\eta}{\beta^2 E_0 T_0}\,V_n \ , \tag{9.117}$$

where d_r is the synchrotron radiation damping rate and the overdot represents derivative with respect to s/v. Here $V_n(s)$ is the total wake voltage seen by bunch n, and is given by

$$V_n(s) = \sum_{p=-\infty}^{\infty}\sum_{k=0}^{M-1} q_k W_0'\left[t_{n,k}^p + \tau_k(s - vt_{n,k}^p) - \tau_n(s)\right] \ , \tag{9.118}$$

where q_k is the charge of bunch k, $t_{n,k}^p = (pM + n - k)T_b$ is the time bunch k is ahead of bunch n p turns ago, and $T_b = T_0/M$ is the bunch spacing[†]. Since the deviation due to synchrotron motion is small compared with the bunch spacing, Eq. (9.118) can be expanded, resulting

$$V_n(s) = \sum_{p=-\infty}^{\infty}\sum_{k=0}^{M-1} q_k\left[\tau_k(s - vt_{n,k}^p) - \tau_n(s)\right] W_0''\left(t_{n,k}^p\right) \ . \tag{9.119}$$

[†]In Eq. (9.9), we have $kC + (s_\ell - s_n)$ in the argument of the wake function W_0', where we are sampling the wake force on the nth bunch due to the ℓth bunch. There, s_n represent the distance along the ring measured from some reference point to the nth bunch in the *same* direction of bunch motion. Thus, the ℓth bunch is ahead of the nth bunch by the distance $s_\ell - s_n$. In Eq. (9.118), we count the number of bunch spacings instead. Thus, the kth bunch is ahead the nth bunch by the time $(n-k)T_b$, since we number the bunches from upstream to downstream or in the *opposite* direction of bunch motion. Note that the term $v(\tau' - \tau)$ in the argument of the linear density in Eq. (9.8) has been neglected because this will only amount to a phase delay $\Omega(\tau' - \tau)$ where $\Omega \approx \omega_s$ and is very much less than the phase change $\omega_r(\tau' - \tau)$.

If all bunches carry the same charge, we have the situation of even fill and the M symmetric eigenmodes are[‡]

$$\boldsymbol{v}_\ell = \frac{1}{\sqrt{M}} \begin{pmatrix} 1 \\ e^{-i\ell\theta} \\ e^{-2i\ell\theta} \\ \vdots \\ e^{-i(M-1)\ell\theta} \end{pmatrix}, \qquad \ell = 0, 1, \cdots, M-1, \qquad \theta = \frac{2\pi}{M} \ . \tag{9.120}$$

They form an orthonormal basis which we called the *even-fill-eigenmode* (EFEM) basis For an uneven fill, it is natural to expand the new eigenmodes using as a basis the EFEMs. The arrival time advances $\tau_n(s)$ for the M bunches in Eq. (9.117) can now be written as

$$\begin{pmatrix} \tau_0 \\ \vdots \\ \tau_{M-1} \end{pmatrix} = \varsigma^0 \boldsymbol{v}_0 + \cdots + \varsigma^{M-1} \boldsymbol{v}_{M-1} \quad \text{or} \quad \tau_n(s) = \frac{1}{\sqrt{M}} \sum_{m=0}^{M-1} \varsigma^m(s) e^{-i2\pi nm/M} \ , \tag{9.121}$$

where the expansion coefficients can be written inversely as

$$\varsigma^m(s) = \frac{1}{\sqrt{M}} \sum_{n=0}^{M-1} \tau_n(s) e^{i2\pi nm/M} \ . \tag{9.122}$$

Assuming the ansatz

$$\tau_k(s) \propto e^{-i\Omega s/v} \ , \tag{9.123}$$

where the collective frequency Ω is to be determined, the voltage from the wake can now be written as

$$V_n(s) = \frac{1}{\sqrt{M}} \sum_{p=-\infty}^{\infty} \sum_{k,m=0}^{M-1} q_k \varsigma^m(s) e^{-i2\pi nm/M} \left[e^{i(m\omega_0+\Omega)t^p_{n,k}} - 1 \right] W_0''(t^p_{n,k}) \ , \tag{9.124}$$

where

$$\varsigma^m(s) \propto e^{-i\Omega s/v} \ . \tag{9.125}$$

[‡]Here, coupled-bunch mode ℓ implies the center-of-mass of a bunch *lags* its predecessor by the phase $2\pi\ell/M$. Thus, coupled-bunch mode ℓ here is the same as coupled-bunch mode $M-\ell$ discussed in the earlier part of this Chapter. There, the center-of-mass of a bunch *leads* its predecessor by the phase $2\pi\ell/M$.

Next project the whole Eq. (9.117) onto the ℓth EFEM, giving

$$\ddot{\varsigma}^{\ell} + 2d_r\dot{\varsigma}^{\ell} + \omega_s^2\varsigma^{\ell} = \frac{e\eta}{\beta^2 E_0 M}\sum_{p=-\infty}^{\infty}\sum_{n,m,k=0}^{M-1}\frac{q_k}{T_0}\varsigma^m(s)e^{i2\pi n(\ell-m)/M}\left[e^{i(m\omega_0+\Omega)t^p_{n.k}}-1\right]W_0''(t^p_{n.k})\ . \quad (9.126)$$

There are too many summations over bunch number. We can eliminate one by defining the integer variable $u = pM + n - k = t^p_{n.k}/T_b$. After that, $\sum_p \to \frac{1}{M}\sum_u$. The summand becomes independent of n and we have $\sum_n = M$. The right side of Eq. (9.126) becomes

$$\text{R.S.} = \frac{e\eta}{\beta^2 E_0 M}\sum_{u=-\infty}^{\infty}\sum_{m=0}^{M-1} I_{l-m}\varsigma^m(s)e^{i2\pi u(\ell-m)/M}\left[e^{i(m\omega_0+\Omega)uT_b}-1\right]W_0''(uT_b)\ , \quad (9.127)$$

where we have introduced the complex amplitude of the pth revolution harmonic in the beam spectrum,

$$I_p = \sum_{k=0}^{M-1} i_k e^{i2\pi kp/M}\ , \quad (9.128)$$

with $i_k = q_k/T_0$ denoting the average current of bunch k. For an evenly filled ring, the average beam current of each bunch is the same. Let us go to the frequency space by introducing the longitudinal impedance,

$$W_0'(t) = \int \frac{d\omega}{2\pi} Z_0^{\parallel}(\omega)e^{-i\omega t}\ . \quad (9.129)$$

The summation over u can now be performed using Poisson formula resulting in the difference of two δ-functions, which facilitate the integration over ω resulting in

$$\text{R.S.} = -\frac{ie\eta}{\beta^2 E_0 T_0}\sum_{p=-\infty}^{\infty}\sum_{m=0}^{M-1} I_{l-m}\varsigma^m(s)\Big\{[(pM+\ell)\omega_0+\Omega]\,Z_0^{\parallel}[(pM+\ell)\omega_0+\Omega] - [(pM+\ell-m)\omega_0]\,Z_0^{\parallel}[(pM+\ell-m)\omega_0]\Big\}\ . \quad (9.130)$$

With the introduction of the coupling impedance,

$$\begin{aligned} Z_{\ell m}(\omega) &= Z_{\text{eff}}\big[\ell\omega_0+\omega\big] - Z_{\text{eff}}\big[(\ell-m)\omega_0\big] \\ Z_{\text{eff}}(\omega) &= \frac{1}{\omega_{\text{rf}}}\sum_{p=-\infty}^{\infty}\big[pM\omega_0+\omega\big]Z_0^{\parallel}\big[pM\omega_0+\omega\big]\ , \end{aligned} \quad (9.131)$$

the equation of motion for the bunches can be written in the simplified form,

$$\ddot{\varsigma}^{\ell} + 2d_r\dot{\varsigma}^{\ell} + \omega_s^2\varsigma^{\ell} = -\frac{ie\eta\omega_{\rm rf}}{\beta^2 E_0 T_0}\sum_{m=0}^{M-1} I_{l-m}Z_{\ell m}(\Omega)\varsigma^m \ . \tag{9.132}$$

The next simplification is to exclude all solutions when $\Omega \approx -\omega_s$ and include only those near $+\omega_s$. From the ansatz (9.123) or (9.125), one has

$$\ddot{\varsigma}^{\ell} + 2d_r\dot{\varsigma}^{\ell} + \omega_s^2\varsigma^{\ell} \approx -2i\omega_s\left[\dot{\varsigma}^{\ell} - (d_r - i\omega_s)\varsigma^{\ell}\right] \ , \tag{9.133}$$

provided that $d_r \ll \omega_s$ and $|\Omega - \omega_s| \ll \omega_s$. We finally obtain

$$\dot{\varsigma}^{\ell} - (d_r - i\omega_s)\varsigma^{\ell} = \sum_{m=0}^{M-1} A_{\ell m}\varsigma^m \ , \tag{9.134}$$

with

$$A_{\ell m} = \frac{e\eta\omega_{\rm rf}}{2\beta^2 E_0 T_0\omega_s} I_{\ell-m}Z_{\ell m}(\omega_s) \ . \tag{9.135}$$

This is just a M-dimensional eigenvalue problem. In the situation of an evenly filled ring, all bunch current i_k are the same and the harmonic spectrum amplitude

$$I_p = \begin{cases} I_0 = \sum_k i_k & p = 0 \\ 0 & p \neq 0 \ , \end{cases} \tag{9.136}$$

where I_0 is the total average current in the ring. This implies no coupling between the EFEMs, as expected, and the eigenvalues are

$$\lambda_\ell = A_{\ell\ell} = \frac{e\eta\omega_{\rm rf}}{2\beta^2 E_0 T_0\omega_s} I_0\left[Z_{\rm eff}(\ell\omega_0 + \omega_s) - Z_{\rm eff}(0)\right] \ , \quad \ell = 1, \ \cdots, \ M-1 \ . \tag{9.137}$$

Some results are apparent:

- The sum of eigenvalues, $\sum A_{\ell\ell}$, is independent of fill shapes.
- Uneven-fill eigenvalues vary linearly as I_0.
- Radiation damping merely shifts all eigenvalues by d_r, regardless of fill shape.
- If all filled buckets have the same charge q_k, then broadband bunch-by-bunch feedback also damps all uneven-fill modes equally, since it behaves like radiation damping.
- The EFEM basis yields a sparse A-matrix because usually coupled-bunch instabilities are driven by only a few parasitic higher-order resonances in the rf cavities.

9.3.4.1 Modulation Coupling

Let us study some special case[§] when $I_k Z_{\rm eff}(k\omega_0) = 0$ except for $k = 0$. This implies that the modulation coupling terms are the only manifestation of fill unevenness. The problem simplifies considerably. In addition, if there is only one sharp resonance exciting instability for mode ℓ in the EFEM basis, this resonance will initiate damping for mode m. We try to couple these two modes by filling the ring unevenly so that $I_{\ell-m}$ is maximized. The A-matrix is now diagonal except for the coupling between these two modes. The coupling A-matrix reduces to a two-by-two matrix. The new eigenvalues for these two modes are

$$\lambda = \frac{1}{2}\left(\lambda_\ell + \lambda_m\right) \pm \frac{1}{2}\sqrt{(\lambda_\ell - \lambda_m)^2 + 4C_{\ell-m}^2 \lambda_\ell \lambda_m}\ , \tag{9.138}$$

where $C_p = |I_p|/I_0$ is called the *modulation parameter* and its value cannot exceed unity. If $C_{\ell-m} = 0$, the even-fill eigenvalues λ_ℓ and λ_m are not perturbed. As $C_{\ell-m}$ approaches unity, one eigenvalue approaches zero and so is its growth rate. The other eigenvalue approaches $\lambda_\ell + \lambda_m$ so that the damping rate of mode m is helping the growth rate of mode ℓ.

To optimize the modulation parameter C_p, we resort to the definition of the harmonic amplitude I_p in Eq. (9.128). As an example, take a ring of $M = 900$ even-fill bunches and we wish to optimize C_p with $p = 3$. According to the definition of the harmonic amplitude I_p in Eq. (9.128), the easiest way to accomplish this is to fill the ring every $M/p = 900/3 = 300$-th bucket (assuming that the total number of bucket is also $M = 900$). Since we wish to keep the same current I_0 in the ring, each of these $p = 3$ chosen buckets will be filled with bunch current $I_0/p = I_0/3$ and the modulation parameter becomes $C_3 = 1$. However, with so much charge concentrated at these 3 buckets, each bunch can become unstable by itself. To cope with this single-bunch instability, we can fill several adjacent buckets around each of these 3 chosen locations. If the maximum allowable bunch current is $i_{\rm max}$, we need to fill up $I_0/(pi_{\rm max})$ adjacent buckets. If $I_0 = 450$ mA and $i_{\rm max} = 2$ mA, we need to fill up 75 adjacent buckets at

[§]Consider a ring with $M = 84$ buckets. If there is a sharp resonance at $\omega_r = (pM + \ell)\omega_0$ with $\ell = 79$, coupled-bunch mode $\ell = 79$ in the EFEM basis will be excited, but mode $m = M - \ell = 5$ will be damped. To couple these two modes, we need to maximize I_k or I_{-k} with $k = \ell - m = 74$. Under this situation, $I_k Z_{\rm eff}(k\omega_0) = 0$ except for $k = 0$, because (1) although $I_{74} \neq 0$, there is no impedance at $(pM \pm 74)\omega_0$, and (2) although $Z_{\rm eff}(k\omega_0) \neq 0$ for $k = \ell$ and $k = m$, I_ℓ and I_m are zero because we maximize $I_{\ell-m}$ only. The same is true if there are a few sharp resonances. This condition, however, excludes the extra Landau damping to be studied in the Sec. 9.3.4.2.

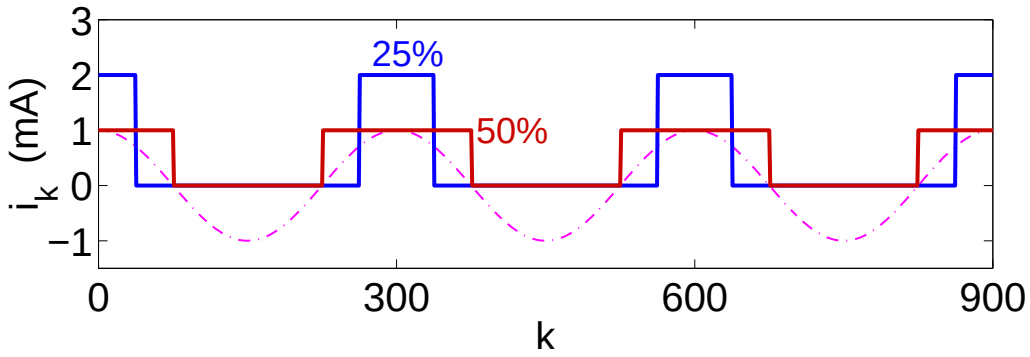

Figure 9.17: (color) Illustration of fill optimization for a ring with $M = 900$ bunches when evenly filled and total beam current $I_0 = 450$ mA. Solid: 50% fill and 25% fill maximize C_3 for $i_{\max} = 1$ mA and 2 mA. Dash-dot: Reference sinusoid at 3 times revolution frequency.

each of the 3 locations. So all in total $x = I_0/(Mi_{\max})$ or 25% of the buckets are filled. If $i_{\max} = 1$ mA instead, 150 adjacent buckets have to be filled in each of the 3 chosen locations, which makes 50% of the ring filled. These patterns are illustrated in Fig. 9.17. When a fraction x of the ring filled in this way, the modulation parameter C_p will be reduced. In general, we can calculate a corresponding "weight" $\cos(2\pi pn/M)$ for each bucket n and fill each of the "heaviest" $I_0/i_{\max}$ buckets to the same current $i_{\max}$. The modulation parameter will be

$$C_p \approx \frac{\sin(\pi x)}{\pi x} \ . \tag{9.139}$$

9.3.4.2 Landau Damping

We need to be a little careful to derive the tune shift for the bunches because, for example, Eq. (9.132) is the equation of motion for a coupled-bunch mode ℓ and not for a particular bunch. We need to use Eq. (9.121) to transform back to the equation of motion of τ_k for bunch k. The frequency shift for bunch k relative to the mean tune is found to be

$$\Delta\omega_s^k = -\frac{ie\eta\omega_{\rm rf}}{\beta^2 E_0 T_0 \omega_s} \sum_{\ell=0}^{M-1} \left[Z_{\rm eff}(\ell\omega_0) I_\ell e^{-i2\pi k\ell/M} \right] \ , \tag{9.140}$$

which is purely real because the real part of the summand is an odd function of ℓ with period M. For an evenly fill pattern, $I_\ell = 0$ unless $\ell = 0$. the tune shift for each bunch will be the same. For $I_\ell \neq 0$ when $\ell \neq 0$, however, different bunches receive different tune shifts, creating a tune spread for Landau damping.

Consider a sharp impedance resonance at $n\omega_0$ which is not a multiple of the bunch frequency $M\omega_0$. If we design a fill optimized for C_n, we excite a sinusoidal ringing in the wake voltage at $n\omega_0$, which contributes to an uneven frequency shift to Eq. (9.140). The larger the modulation parameter the larger will be the tune spread. Figure 9.18 shows the increase in Landau damping as the fill fraction x is decreased. In the figure, $\mathcal{R}e\,\lambda$ is proportional to the growth rate while $\mathcal{I}m\,\lambda$ is proportional to the tune shift. Interestingly, eigenvalues with large imaginary parts are completely damped even by 80% fills.

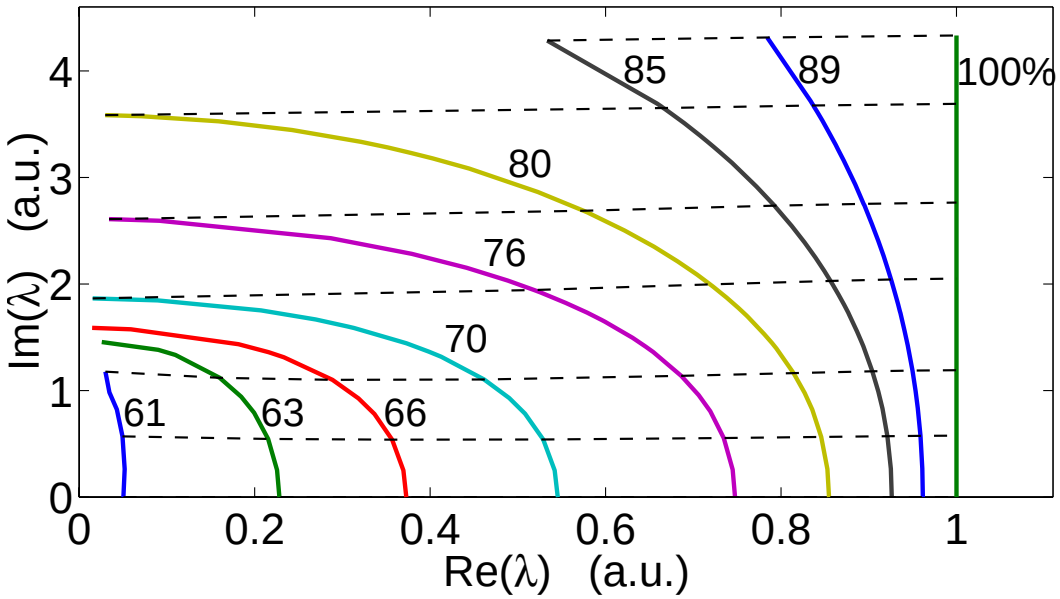

Figure 9.18: (color) Graphic look-up table for fill-induced damping of eigenvalue of unstable longitudinal EFEM n as C_n is increased from 0 (100% of ring filled) to 0.5 (61% filled). Dashes: Evolution of λ_n from a few even-fill starting points.

9.3.4.3 APPLICATION

There are longitudinal coupled-bunch instabilities in the PEP-II Low Energy Ring (LER) at $I_0 = 1$ A and $M = 873$ [14]. The two largest cavity resonances are expected to drive bands of modes centered at 93.1 MHz (EFEM 683) and 105 MHz (EFEM 770) unstable. They also stabilize the corresponding bands at 25.9 MHz (EFEM 190) and 14 MHz (EFEM 103). The growth and damping rate spectrum are shown in Fig. 9.19(a). The best modulation-coupling cure is to couple the modes around 105 MHz to those near 25.9 MHz by maximizing C_{580} or C_{293} ($C_p = C_{M-p}$). This will automatically couples

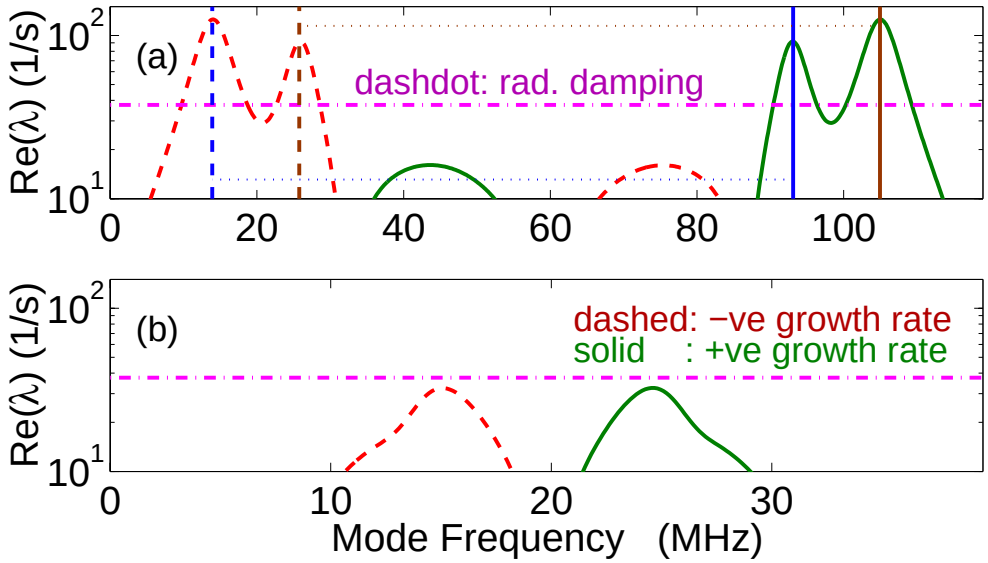

Figure 9.19: (color) Illustration of fill optimization for a ring with $M = 1000$ bunches when evenly filled and total beam current $I_0 = 500$ mA. Solid: 50% fill and 25% fill maximize C_4 for $i_{\max} = 1$ mA and 2 mA. Dash-dot: Reference sinusoid at 4 times revolution frequency.

93.1 MHz to 14 MHz. The optimization can be easily accomplished by filling every third nominally-spaced bucket, since $873/3 = 291$ is close to 293. This is equivalent to slicing the frequency range from zero to $M\omega_0$ and placing the three parts of the growth or damping spectrum on each other. Thus the damping parts will help the growing parts. The calculation illustrated in Fig. 9.19(b) shows that such a fill should be stable at 1 A.

Modulation coupling was expected to raise the instability threshold from 305 mA (nominal spacing) to 1.16 A (3 times nominal spacing). The measured thresholds are 350 mA and 660 mA, respectively.

Theoretical predictions of fill-induced Landau damping were first tested at the Advanced Light Source (ALS). Only two of the 328 ALS modes were unstable: mode 204 and 233. The effective impedance at $233\omega_0$ was used to create a tune spread by maximizing C_{233}.

A baseline even-fill instability measurement was first made at $I_0 = 172$ mA. This gave the two eigenvalues $\lambda_{204} = (0.47 \pm 0.02) + i(0.05 \pm 0.03)$ ms^{-1} and $\lambda_{233} = (0.61 \pm 0.02) + i(1.16 \pm 0.03)$ ms^{-1}, assuming that the radiation damping rate $d_r = 0.074$ ms^{-1}. It is evident from Fig. 9.18 that fill fraction less than 60% will damp the target mode almost completely. Thus, any residual instability in the Landau fill must correspond to

the Landau-damped mode 204. Numerical calculation gives us only one unstable mode with eigenvalue $(0.1 \pm 0.04) - i(1.62 \pm 0.06)$ ms^{-1}, whose real part is about 6 times less than in the even-fill case. The measured eigenvalue for a 175-mA beam with $C_{233} = 0.67$ is $(0.09 \pm 0.003) - i(1.63 \pm 0.005)$ ms^{-1}, in agreement with the theoretical prediction.

Prediction of uneven fill has also been made on the light source at SRRC of Taiwan [15]. The main source of longitudinal impedance is from the Doris type rf cavities, which have a resonance at 744.1948 MHz, loaded $Q_L = 2219$ and $R_L/Q_L = 31.95\ \Omega$. But from the observation on the real machine, the unstable mode number is 97 or resonance frequency is 742 MHz. There are $M = 200$ rf bucket in the SRRC ring. Thus, the most stable mode is 103. To couple the two modes, one must maximize C_6, or the filling pattern is in 6 groups of buckets. The simulations consist of using three uneven fill patterns as illustrated on the left side of Fig. 9.20 with a total beam current of 200 mA.

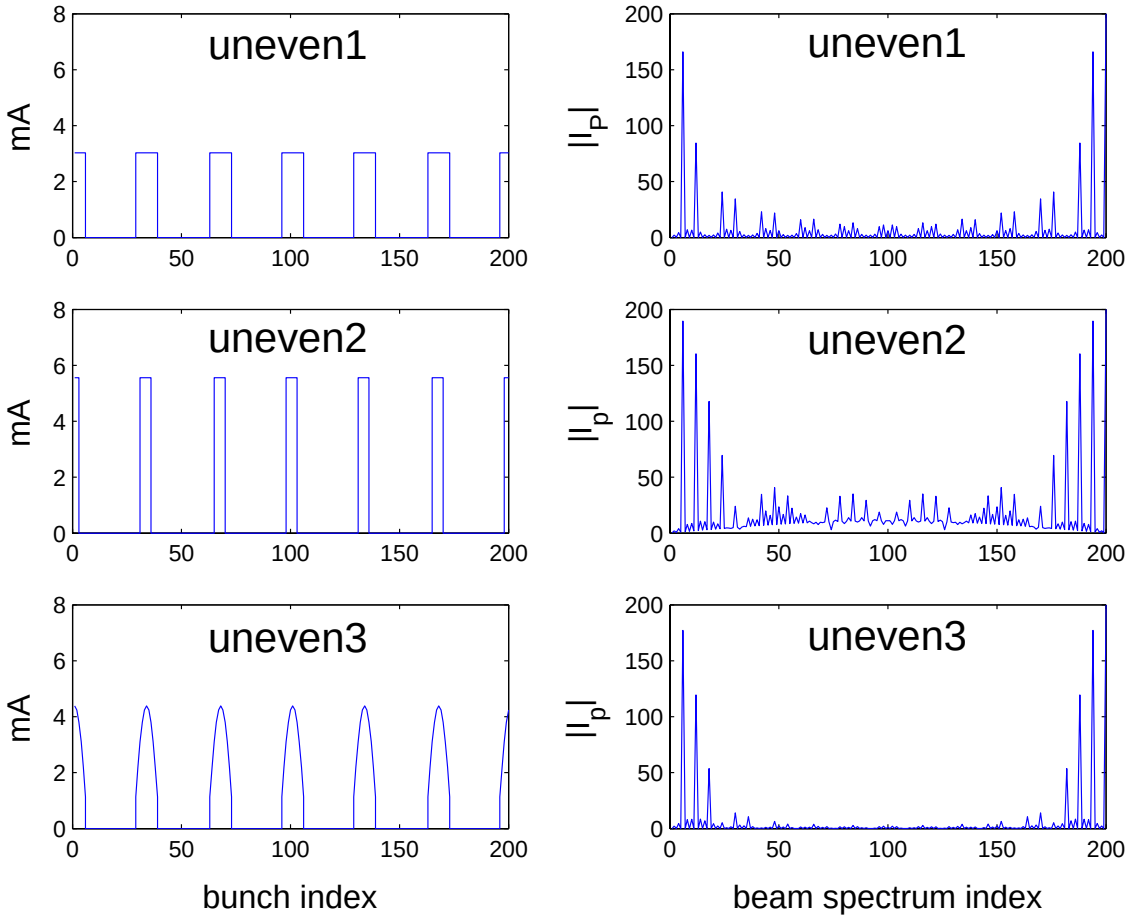

Figure 9.20: Fill patterns used in the simulation of the Taiwan Light Source.

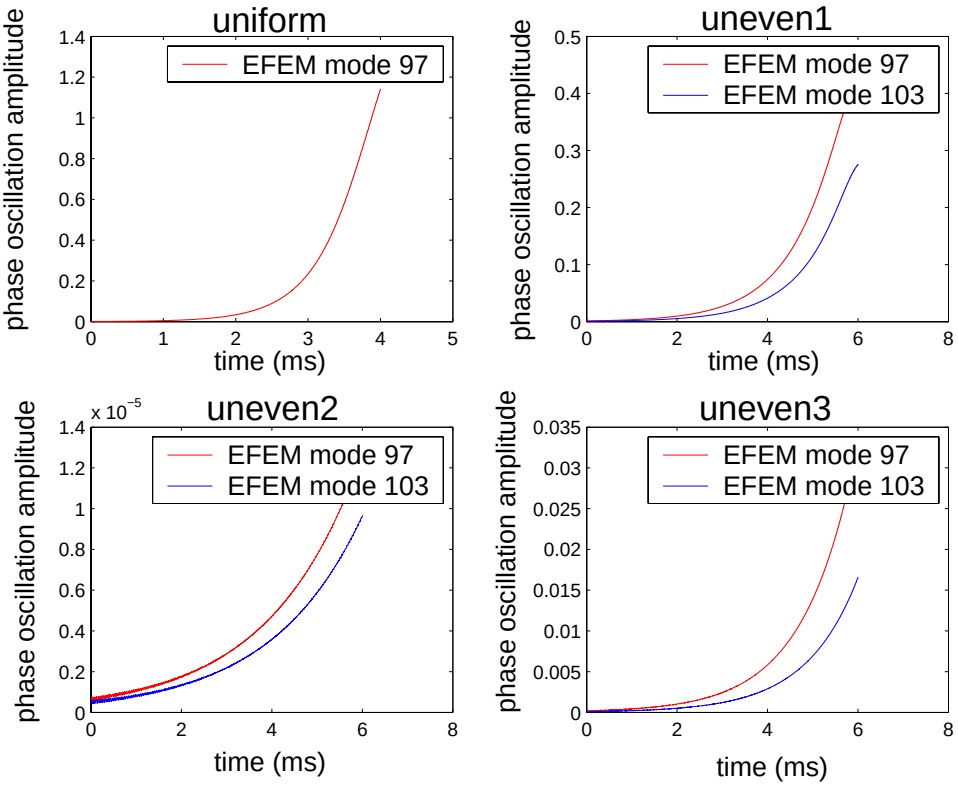

Figure 9.21: (color) The evolution of EFEM 97 and EFEM 103 of four fill patterns from simulation.

Table 9.1: Simulation results of growth rates of EFEM 97 and 103 of four fill patterns. 5 ms radiation damping time has been included.

Fill pattern	C_6	Growth rate ms^{-1}	
		EFEM 97	EFEM 103
uniform	0	1.9399	—
uneven1	0.8302	1.0004	1.0182
uneven2	0.9476	0.4947	0.4947
uneven3	0.8855	0.8659	0.8703

The spectra are shown on the right side. The growth rates for the two modes are displayed in Fig. 9.21 and listed in Table 9.1. Note that the derived growth rates include 5 ms radiation damping time. We see that the uneven fills do help to damp the beam instability, although the result has not been completely satisfactory because the instability still grows.

9.4 Exercises

9.1. Above/below transition, with the angular resonant frequency ω_r offset by $\Delta\omega = \pm(\omega_r - h\omega_0)$ where $\omega_{\rm rf} = h\omega_0$ is the angular rf frequency, h is the rf harmonic, and ω_0 is the revolution angular velocity, the bunch suffers Robinson's instability.
(1) Assuming that $\omega_s \ll |\Delta\omega| \ll \omega_{\rm rf}$ and using the expression for resonant impedance in Eq. (1.40), show that the Robinson's growth rate in Eq. (9.41) can be written as

$$\frac{1}{\tau} = -\frac{2e^2 N\eta R_s Q}{\beta^2 E_0 T_0^2}\cos^2\psi\sin 2\psi \ , \tag{9.141}$$

where N is the number of particles in the bunch, E_0 is the synchronous energy, βc is the velocity of the synchronous particle with c being the velocity of light, $T_0 = 2\pi/\omega_0$ is the revolution period, η is the slip factor, and the detuning angle ψ is defined as

$$\tan\psi = 2Q\frac{\omega_r - \omega_{\rm rf}}{\omega_r}$$

for the resonant impedance with shunt impedance R_s, resonant frequency $\omega_r/(2\pi)$, and quality factor Q.
(2) Assuming further that $|\Delta\omega|$ is much less than the resonator width $\omega_r/(2Q)$ which, in turn, is much less than ω_0, show that the Robinson's growth rate can be written as

$$\frac{1}{\tau} = -\frac{4e^2 N R_s Q^2\eta\Delta\omega}{\pi\beta^2 E_0 h T_0} \ . \tag{9.142}$$

(3) Robinson instability is usually more pronounced in electron than proton machines because high shunt impedance and quality factor are often required in the rf system. Take for example a ring of circumference 180 m with slip factor $|\eta| = 0.03$. To store a typical bunch with 1×10^{11} electrons at $E_0 = 1$ GeV, one may need an rf system with $h = 240$, $R_s = 1.0$ MΩ, and $Q = 2000$. On the other hand, to store a bunch of 1×10^{11} protons at kinetic energy $E_0 = 1$ GeV in the same ring, one may need an rf system with $h = 4$, $R_s = 0.12$ MΩ, and $Q = 45$. Compare the Robinson's growth rates for the two situations when the resonant frequencies are offset in the wrong directions by $|\Delta\omega| = \omega_s$. Assume the synchrotron tune to be 0.01 in both cases.

9.2. From Eq. (3.50), derive the potential-well contribution to the coherent synchrotron tune shift of a short bunch in the dipole mode. Show that this static contribution just cancels the dynamical contribution in Eq. (9.35) when the driving impedance is broadband.

9.3. Using the definition of the form factor in Eq. (9.68), compute numerically the form factor when the unperturbed distribution is bi-Gaussian. The half bunch length can be taken as $\hat{\tau} = \sqrt{6}\sigma_\tau$, where σ_τ is the rms bunch length.

9.4. Consider a single sinusoidal rf system operating at synchronous angle $\phi_s = 0$.
(1) Show that the synchrotron frequency of a particle at rf phase ϕ is given by

$$\frac{f_s(\phi)}{f_{s0}} = \frac{\pi}{2K(t)} \,, \tag{9.143}$$

where $t = \sin\phi/2$, f_{s0} is the synchrotron frequency at zero amplitude, and $K(t)$ is the complete elliptic integral of the first kind defined in Eq. (9.80).
(2) Show that Eq. (9.143) is consistent with Eq. (9.51) at small amplitudes.

9.5. Solve the set of equations in Eqs. (9.75) to (9.77) to obtain the fundamental rf phase ϕ_s, the higher-harmonic rf phase ϕ_m and the voltage ratio r in terms of the harmonic ratio m and $U_s/eV_{\rm rf}$.
Answer:

$$\sin\phi_s = \frac{m^2}{m^2-1}\frac{U_s}{eV_{\rm rf}} \,, \quad \tan\phi_m = \frac{\dfrac{m}{m^2-1}\dfrac{U_s}{eV_{\rm rf}}}{\sqrt{1-\left(\dfrac{m^2}{m^2-1}\dfrac{U_s}{eV_{\rm rf}}\right)^2}} \,, \quad r = \sqrt{\frac{1}{m^2} - \frac{1}{m^2-1}\frac{U_s^2}{(eV_{\rm rf})^2}} \,.$$

9.6. Derive the small-amplitude synchrotron frequency as given by Eq. (9.79).

Bibliography

[1] P.B. Robinson, *Stability of Beam in Radiofrequency System*, Cambridge Electron Accel. Report CEAL-1010, 1964.

[2] F.J. Sacherer, *A Longitudinal Stability Criterion for Bunched Beams*, CERN report CERN/MPS/BR 73-1, 1973; IEEE Trans. Nuclear Sci. **NS 20**, 3, 825 (1973).

[3] R.D. Kohaupt, DESY Report No. DESY 85-139,1985.

[4] S. Prabhakar, *New Diagnostic and Cures for Coupled-Bunch Instabilities*, Ph.D. thesis, Stanford University, 2000, 1999, SLAC Preprint SLAC-R-554.

[5] A. Hofmann and S. Myers, *Beam Dynamics in a Double RF System*, Proc. 11th Int. Conf. High Energy Accel., Geneva, 1980.

[6] A. Mosnier, *Cures of Coupled Bunch Instabilities*, PAC'99, Paper FRBR2.

[7] S.Y. Lee *et al*, Phys. Rev. **E49**, 5717 (1994); J.Y. Liu *et al*, Phys. Rev. **E50**, R3349 (1994): J.Y. Liu *et al*, Part. Accel. **49**, 221-251 (1995).

[8] R. Averill *et al.*, Proceedings of 8th International Conference on High Energy Accelerators, CERN (1971) p. 301.

[9] P. Bramham *et al.*, Proceedings of 9th International Conference on High Energy Accelerators, CERN (1974); P. Bramham *et al.*, IEEE Trans. Nucl. Sci. **NS-24**, 1490 (1977).

[10] J.M. Baillod *et al.*, IEEE Trans. Nucl. Sci. **NS-30**, 3499 (1983); G. Galato *et al.*, Proceedings of the IEEE Particle Accel. Conference, 1987, p. 1298.

[11] D. Li, M. Ball, B. Brabson, J. Budnick, D.D. Caussyn, A.W. Chao, V. Derenchuk, S. Dutt, G. East, M. Ellison, D. Friesel, B. Hamilton, H. Huang, W.P. Jones, S.Y. Lee, J.Y. Liu, M.G. Minty, K.Y. Ng, X. Pei, A. Riabko, T. Sloan, M. Syphers, Y. Wang, Y. Yan, and P.L. Zhang, '*Effects of Rf Voltage Modulation on Particle Motion*, Nucl. Inst. Meth. **A364**, 205 (1995).

[12] M.H. Wang, Peace Chang, P.J. Chou, K.T. Hsu, C.C. Kuo, J.C. Lee, and W.K. Lau, *Experiment of RF Voltage Modulation at at SRRC*, PAC'99, Paper THA106.

[13] K.Y. Ng, *Damping of Coupled-Bunch Growth by Self-Excited Cavity*, Fermilab Internal Report FERMILAB-FN-456, 1987; K.Y. Ng, *Longitudinal Coupled-Bunch Instability in the Fermilab Booster*, Fermilab Internal Report FERMILAB-FN-464, 1987 (KEK Report 87-17).

[14] S. Prabhakar, *New Diagnostic and Cures for Coupled-Bunch Instabilities*, Proceedings of the IEEE Particle Accel. Conference, Chicago, 2001.

[15] M.H. Wang, P.J. Chou, and A.W. Chao, *Study of Uneven Fills to Cure the Coupled-Bunch Instability in SRRC*, Proceedings of the IEEE Particle Accel. Conference, Chicago, 2001.